Application of Smart Antennas to Wideband Code Division Multiple Access : the Uplink Performance

by

Don N. Wijayasinghe

A Thesis submitted to the Faculty of Engineering, Science and Technology of the Victoria University of Technology in fulfillment of the requirements of the degree of Master of Engineering.

School of Electrical Engineering
Victoria University of Technology
Melbourne, Australia

March 2004

Declaration

I conducted my research studies under the guidance of Associate Professor Fu-Chun Zheng and Professor Mike Faulkner. Some of the results reported in this thesis have been published as academic papers in international conferences. These papers are:

1. D.N. Wijayasinghe and F.C. Zheng, " The Performance Evaluation of a Smart Antenna Receiver for WCDMA", *IEEE Region 10 Conference on Convergent Technologies (TENCON)*, pp. 1590-1594, Bangalore, India, October, 2003.

2. D.N. Wijayasinghe and F.C. Zheng, " Smart Antennas for WCDMA", *Proc. of the Fourth International Conference on Modelling and Simulation*, pp. 174-179, Melbourne, Australia, November, 2002.

I hereby declare that the contents of this thesis are the results of my own work except where references are made.

Don N. Wijayasinghe

Telecommunication and Micro-Electronics Group
School of Electrical Engineering
Faculty of Engineering, Science and Technology
Victoria University of Technology
Melbourne
Australia

List of Abbreviations

2G	Second Generation
3G	Third Generation
3GPP	Third Generation Partnership Project
AMI	Adaptive Matrix Inversion
AOA	Angle Of Arrival
AWGN	Additive White Gaussian Noise
BER	Bit Error Rate
BPSK	Binary Phase Shift Keying
CDF	Cumulative Density Function
CDMA	Code Division Multiple Access
CFA	Code Filtering Approach
CGA	Code Gated Algorithm
CMA	Constant Modulus Algorithm
DD	Decision Directed
DFT	Discrete Fourier Transform
DOA	Direction of Arrival
DPCCH	Dedicated Physical Control Channel
DPCH	Dedicated Physical Channel
DPDCH	Dedicated Physical Data Channel
DSP	Digital Signal Processor
EIRP	Effective Isotropic Radiated Power
FBI	Feed Back Information
FCC	Federal Communication Council
FDD	Frequency Division Duplex
GE	Genaralised Eigenvalue
GLM	Generalised Lagrange Multiplier

GPM	Generalised Power Method
HPF	High Pass Filter
LES	Linear Equally Spaced
LM	Lagrange Multiplier
LMS	Least Mean Squares
LOS	Line Of Sight
LPF	Low Pass Filter
LS-CMA	Least Squares Constant Modulus Algorithm
LS-DRMTA	Least Squares De-spread Re-spread Muti Target Array
MAC	Medium Access Control
MEM	Maximum Entropy Method
MSINR	Maximum Signal to Interference and Noise Ratio
MUSIC	Multiple Signal Classification
PDF	Probability Density Function
PSA	Pilot Symbol Assisted
QPSK	Quadrature Phase Shift Keying
RF	Radio Frequency
RLC	Radio Link Control
RLS	Recursive Least Squares
SB	Switched Beam
SCORE	Self Coherence Restoral
SDMA	Space Division Multiple Access
SF	Spreading Factor
SIR	Signal to Interference Ratio
SLA	Spectral Line Approximation
SNR	Signal to Noise Ratio
SVD	Singular Value Decomposition
TDD	Time Division Duplex
TDMA	Time Division Multiple Access

TFCI	Transport Format Combination Indicator
TPC	Transmit Power Control
UTRA	UMTS Terrestrial Radio Access
WCDMA	Wide Band Code Division Multiplex Access

List of Tables

List of Figures

Acknowledgements

I would like to express my sincere gratitude to Associate Professor Fu-Chun Zheng for his support and advice throughout the term of this research.

I wish to thank my co-supervisor Professor Mike Faulkner for his valuable suggestions.

I am also grateful to the telecommunications and micro-electronics team and the technical staff for their support in numerous instances.

Last but not least, I give my deepest appreciation to the members of my family for their love, support and encouragement.

Abstract

Adaptive antenna arrays have recently been introduced to cope with the high capacity required by the 3rd generation (3G) wireless communications systems. As adaptive antenna arrays focus narrow high gain beams towards the desired user and nulls towards interferers, both coverage and capacity of the network can be improved. To establish the performance gain that a smart antenna can deliver in a 3G environment (i.e., with mixed traffic), the implementation of adaptive antenna arrays for the uplink of a Wideband Code Division Multiple Access (WCDMA) system in the Frequency Division Duplex (FDD) mode is addressed in this thesis.

The beam-forming is implemented with a LS-DRMTA algorithm and a Lagrange multiplier based algorithm using the Q channel only. The results show that the adaptive antenna arrays offer significant performance enhancement over switched beam and single antennas in a 3G environment (i.e., with mixed traffic).

Contents

Chapter 1

Introduction

The 3rd generation mobile systems (3G) are designed to support multimedia communications that is capable of integrating a wide variety of communication services such as high quality images, video, multimedia traffic as well as voice. To accomplish the 3G mobile system requirements, WCDMA (Wideband Code Division Multiple Access) has emerged as the most widely adopted third generation air interface. The specifications for W-CDMA have been created by the 3GPP group, consisting of the standardization bodies from Europe, Japan, Korea, the US and China. One of the main requirements in 3G is to increase capacity, coverage and cost effectiveness while keeping the quality of service at a higher level. Smart antennas have been suggested as a potential option to accomplish the above 3G requirements.

1.1 Basic Principles of Smart Antennas

Smart antennas are defined in several ways in literature. The most widely used definition is that a smart antenna has an adaptive radiation pattern compared with a conventional antenna, which has a fixed radiation pattern. Normally, a smart antenna consists of a number of radiating elements, a combining/dividing network and a control unit. The intelligence of the smart antenna is located in the control unit, which is realized using a Digital Signal Processor (DSP). The feeder parameters of the antennas are controlled by the DSP in order to optimize the communications link. There are different optimization techniques, some of which will be discussed later in the thesis.

The output signal at the array is produced by combining each antenna signal with a weight factor. As a result, a smart antenna can dynamically generate multiple beam and null patterns in a particular direction. Theory behind smart antennas is not new and has been used in radar and aerospace technology for many years. Until recent years, however cost effectiveness has prevented their use in commercial systems. In particular, the availability of low cost and very fast digital signal processors has made smart antennas practical for land and satellite mobile communications systems. In a mobile communications network, the interferers rarely have the same geographical location as the user. Therefore, by maximizing the antenna gain in the direction of the desired user and simultaneously placing nulls in the directions of the interferers, the quality of the communications link can be significantly improved.

1.2 Types of Smart Antennas

Smart antennas are broadly categorized into two types: switched beam arrays and adaptive arrays. The mode of operation of a switch beam antenna is simple: it selects one of the predefined beams of the array at a time by using a switching function. The beam that gives the highest received power is employed as the best beam at any given time. This type of antennas can be implemented in existing networks more easily than the more complicated adaptive arrays. On the other hand the operation of adaptive array systems is different from that of switched beam systems: they continually monitor their coverage area in order to adapt to their changing radio environment. The radiation pattern is adjusted to direct the main beam towards the desired user and nulls towards the interferers. Moreover, by using beamforming algorithms and space diversity techniques, the radiation pattern can be adapted to receive multi-path signals, which can then be combined. Both of these smart antenna types are analyzed in more detail later in the thesis.

1.3 Smart Antennas: Benefits and Costs

The application of smart antennas will have a significant impact on the performance of the existing and future mobile networks. This section will outline the potential benefits and cost effectiveness of using smart antennas in mobile networks.

(a) Capacity Increase

The main advantage of using smart antennas in mobile networks is the capacity increase. Typically, signal to interference ratio (SIR), in a mobile network is much higher than the signal to thermal noise ratio (SNR). When smart antennas are employed, the interference will be suppressed, leading to a higher SIR, and therefore a higher capacity. The application of smart antennas in both TDMA and CDMA systems has shown that an increase of capacity can indeed be obtained. In TDMA systems, the higher capacity is achieved as a result of reduced frequency reuse distance due to the increased SIR. In CDMA systems, more capacity can be expected compared with TDMA systems. This is because CDMA systems are more inherently interference-limited than TDMA systems. In fact, the main source of interference in the CDMA system is the interference from other users due to the spreading codes being non-ideally orthogonal.

(b) Range Increase

Radio coverage, rather than capacity is a significant consideration in base station deployment in rural areas. Since smart antennas will be more directive than conventional antennas, a range increase is possible with smart antennas. Therefore, base stations can be deployed further apart, leading to a more cost effective solution.

(c) New Services

A mobile network with smart antennas has the potential of providing more accurate spatial information about the user than the existing networks. Information about user position is useful in providing services such as emergency response, location-specific billing etc. This user location capability has become compulsory in United States to comply with the FCC requirement.

(d) Security

A network is more difficult to tap when smart antennas are used. This is because the radiation is directional towards the user and it is hard to place the eavesdropper in the same direction as the user.

(e) Cost Considerations

The cost is a significant factor that has to be evaluated against the benefits.

(f) Complexity of the Transceiver

Since smart antennas use sophisticated beamforming techniques, smart antenna transceiver is in general much more complex than a conventional transceiver. In other words, smart antennas employ powerful numeric processors and control systems, which increases the cost of the smart antennas.

(g) Resource Management

A network with smart antennas uses either interference suppression or Space Division Multiplex Access (SDMA). The latter means that different users use the same physical communication channel in the same cell, separated only by their respective angles of arrival. Therefore, systems adapting full SDMA will need more intra-cell handovers than the conventional systems (TDMA or CDMA systems). Hence more resource management is required for networks with smart antennas.

(h) Physical Size

As the demand for smaller physical size of the base station antenna is growing even from existing networks, smart antennas with typical sizes varying from 4 to 12 elements could create a drawback.

1.4 Motivation for the Research

Traditional antenna systems deployed in wireless networks are designed to radiate RF (Radio Frequency) energy only to achieve the desired coverage characteristics. These systems cannot change beam patterns dynamically to cater for the changing traffic requirements. Smart antennas are a new technology to overcome these limitations and they are possible to be engineered to form a movable beam pattern by means of either DSP (Digital Signal Processing) or RF hardware to a desired direction (the user direction). This will effectively reduce the interference within the mobile network. Therefore, the significance of this research can be outlined as follows.

- Smart antennas will increase the capacity of existing networks as well new ones as a result of their interference reduction capability.

- As smart antennas focus radiation beams towards the desired user, the effective coverage area of the cell site will be increased.

- In a mixed data rate environment, the focused beam of the smart antenna towards the desired user will lead to an increase in EIRP (Effective Isotropic Radiated Power), which saves transmit power.

1.5 Objectives of the Research

The overall aim of this research is to examine techniques that will enhance the performance of smart antenna receivers at the uplink of a WCDMA system in the frequency division duplex mode (FDD). This involves the following specific aims:

- To explore efficient adaptive algorithms based on maximum SINR (Signal to Interference and Noise Ratio) criteria to be used in smart antenna receivers.

- To compare the BER (Bit Error Rate) performance of the smart antenna receivers with the conventional receivers.

- To investigate further performance enhancement techniques for smart antenna receivers using specific methods such as Lagrange Multiplier method.

1.6 Thesis Breakdown

The rest of this thesis has been organized into the following six chapters.

- Chapter 2: WCDMA

Chapter 2 starts with a discussion of the characteristics of WCDMA air interface, which includes WCDMA physical layer, physical channel structure and specifications for multi-rate data transmission.

- Chapter 3: Smart Antenna Algorithms

This Chapter summarises the current developments of smart antennas and some smart antenna algorithms presented in the literature.

- Chapter 4: Simulation Models

Chapter 4 describes the methodology adapted in implementing the simulation program. It contains three main sections: transmitter, channel model and receiver. The Spatial channel model and Rayleigh fading channel model are presented in detail. Clarke's model is used to develop Rayleigh fading simulation program.

- Chapter 5: Smart Antennas

This chapter presents a detail description and analysis of smart antennas, which include both switched beam antennas and adaptive array antennas. Adaptive algorithm is an important part of adaptive antennas. Two adaptive algorithms based on LS-DRMTA and Lagrange Multiplier are discussed in this chapter.

- Chapter 6: Performance Comparison Results

A comprehensive analysis of the simulation results is presented in this chapter. The simulation results are given in terms of Bit Error Rate (BER), radiation plots and pole capacity. The performance of the adaptive antenna arrays is also compared with the switched beam and omni directional antennas.

- Chapter 7: Conclusion and Future Work

Chapter 7 summarises the results of the research and also suggests some further areas for future investigation.

Chapter 2

WCDMA

2.1.Introduction

This chapter presents the basic principles of WCDMA air interface that will form the basis for this research project. WCDMA air interface, referred to also as UMTS terrestrial radio access (UTRA), was developed and continuously updated by the third generation partnership project (3GPP). WCDMA has two modes of operation: frequency division duplex (FDD) and time division duplex (TDD). A brief description of FDD and TDD modes is given as follows:

FDD : In this duplex method, the uplink and downlink transmission employ two separated frequency bands. A user is assigned a pair of frequency band with a specified separation.

TDD : In this duplex method, uplink and downlink transmission are carried over the same frequency band by using synchronised time intervals. Thus time slots in a physical channel are divided into transmission and reception parts.

WCDMA, as its name implies, is a code division multiple access (CDMA) system. In CDMA, all users transmit at the same time as opposed to time division multiple access (TDMA). Frequency divisions are still used, but at a much larger bandwidth. Further more, multiple users share the same frequency carrier and each user's signal uses a unique code that appears to be interference to all except the desired receiver. Correlation techniques allow a receiver to decode one signal among many that are transmitted on the same carrier at the same time. Unlike some second generation (2G) and 3G CDMA systems, WCDMA does not require an external time synchronization source such as the Global Positioning System (GPS). A nominal bandwidth of 5MHz has been proposed for all 3G applications. Three main reasons have been given for choosing this bandwidth. First, the main target data rates of 3G: 144 and 384 kbps are achievable within the 5MHz bandwidth. Second, 3G systems are to be deployed within the existing frequency bands occupied already by 2G systems. Third, performance can be improved by the larger 5MHz bandwidth resolving more multipaths than narrower bandwidths, increasing diversity [22].

WCDMA air interface is characterised by the following key features:

- Support of high rate transmission: 384kbps with wide area coverage, 2Mbps with local coverage.
- Provision of multirate services.
- Packet data.
- Seamless inter frequency hand over.
- Fast power control in the downlink.
- Complex spreading.
- Built in support for future capacity and coverage enhancing technologies like adaptive antennas, advanced receiver structures and transmitter diversity.

2.2 WCDMA specifications

The air interface based on the 3GPP WCDMA specifications can be summarised using the following table.

Channel bandwidth	5MHz
Duplex mode	FDD and TDD
Chip rate	3.84 Mbps
Frame length	10 ms
Spreading modulation	Balanced QPSK (down link) Dual channel QPSK (uplink) Complex spreading
Data modulation	QPSK (downlink) BPSK (uplink)
Channel coding	Convolutional and turbo coded
Coherent detection	User dedicated time multiplexed pilot (downlink and uplink), common pilot in the downlink
Channel multiplexing in downlink	Data and control channels time multiplexed
Channel multiplexing in uplink	Control and pilot channel time multiplexed I & Q multiplexing for data and control channel
Multi-rate	Variable spreading and multi-code

Spreading factors	4-256 (uplink), 4-512 (downlink)
Power control	Open and fast closed loop (1.6 kHz)
Spreading (downlink)	OVSF sequences for channel separation Gold sequences 2^{18}-1 for cell separation (truncated cycle 10ms)
Spreading (uplink)	OVSF sequences, Gold sequence 2^{41} for user separation (different time shifts in I and Q channel, truncated cycle 10ms)
Hand over	Soft handover Inter-frequency handover
Downlink RF channel structure	Direct spread

Table 2.1: WCDMA specifications.

2.3 Protocol Architecture

As shown in Fig.2.2 the protocol architecture is organised into three protocol layers[22]:

- The physical layer (L1)
- The data link layer (L2)
- The Network layer (L3)

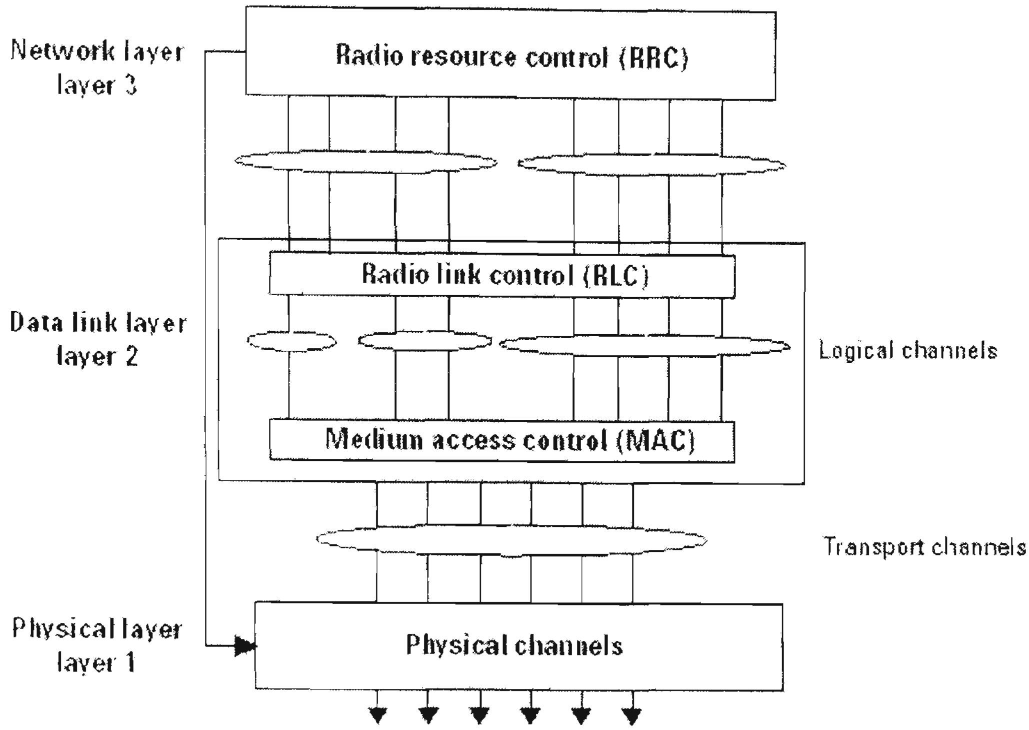

Figure 2.2: WCDMA protocol structure[22].

The network layer (L3) is responsible for connecting services from the network to user equipment (UE). The data link layer (L2) consists of two functional blocks: the medium access control (MAC) and the radio link control (RLC) blocks. The RLC is responsible for the transfer of user data, error correction, flow control, protocol error detection and recovery, and ciphering. The MAC sublayer is responsible for mapping between logical channels and transport channels. Also MAC sublayer provides data transfer services on logical channels. The physical layer is responsible for mapping the transport channels onto the physical channels and performs all of the Radio Frequency (RF) functions necessary to make the system work. These RF functions include: frequency and time synchronization, rate matching, spreading and modulation, power control, and soft handoff. This research focuses on the WCDMA physical layer, which will be presented in the next section, and more information on the other layers can be found in 3GPP specifications (***www.3gpp.org***).

2.4 WCDMA Physical Layer

The following sub-sections are devoted to describing the physical layer of the radio access network of a WCDMA system operating in the FDD mode. The spreading and the scrambling operations of the Dedicated Physical Channel (DPCH) for the uplink will be discussed as they play a major role in our simulations that will be presented in chapter 4. The down link operation is not discussed as it is beyond the scope of this project. For a detailed description of the physical layer, one should refer to the 3GPP documentation [5,30].

Physical Channel Structure

The physical channels of a WCDMA consist of two channels for both uplink and down link.

(1). Dedicated Physical Data Channel (DPDCH): it functions as a carrier for dedicated data generated at Layer 2 and above.

(2). Dedicated Physical Control Channel (DPCCH): it functions as a carrier for Layer 1 control bits.

2.4.1 Frame Structure for Uplink

As is shown in the figure below, the principal frame structure of the uplink dedicated physical channel consists of one super frame, which is divided into 72 frames of 10ms each. Each frame is split into 15 slots, each of which has a length of 2560 chips corresponding to one power control period.

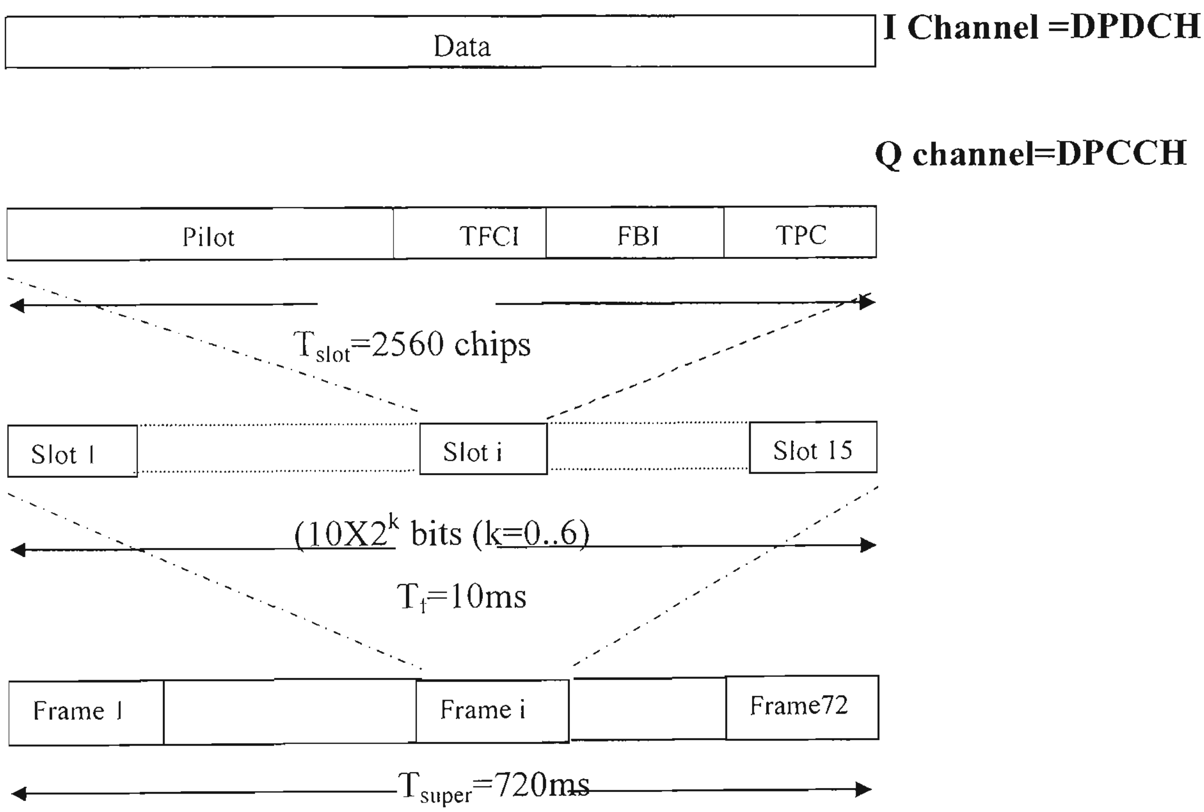

Figure 2.3: Frame structure for uplink DPDCH/DPCCH.

As indicated above, each slot consists of the Pilot, TFCI, FBI and TPC bits. Their definitions and specific usage may be briefly described as follows:

Pilot bits: assisting coherent demodulation and channel estimation.

TFCI bits: (Transport Format Combination Indicator) used to indicate and identify several simultaneous services.

FBI bits: (Feedback Information) used to support techniques requiring feedback.

TPC bits: (Transmit Power Control) used for power control purposes.

The number of bits in each slot is derived from the parameter k given in Fig. 2.3 and it relates to the spreading factor of the physical channel by the relationship:

$$SF = \frac{256}{2^k}.$$

When k varies from 0 to 6, the spreading factor varies from 256 to 4. The spreading factor is determined by the desired data rate of the channel.

2.5 Multirate Data Transmission

WCDMA is a technology that enables flexible multi-rate transmission. That means WCDMA is capable of supporting different types of service using different data rates and quality of service parameters. This is achieved by encoding data from transport channels and then mapping to the physical channels and transmitting over the air interface. The channel-coding scheme is a combination of error correction coding, rate matching, interleaving and channel mapping [22]. Uplink data rates for DPDCH are given in the table below.

DPDCH Spreading Factor	DPDCH Bit rates (kbps)	Maximum user data rate with ½ rate coding (approx.)
256	15	7.5 kbps
128	30	15 kbps
64	60	30 kbps
32	120	60 kbps
16	240	120 kbps
8	480	250 kbps
4	960	480 kbps
4, with 6 parallel codes	5740	2.3 Mbps

Table 2.4: Uplink data rates for DPDCH.

Chapter 3

Smart Antenna Algorithms

3.1 Introduction

The smart antenna technology for mobile communication has gathered enormous interest and attention during the last few years. This is due to the advances in flexible algorithms at the receiver and transmitter in communication systems. Different levels of intelligence have been introduced to the smart antennas ranging from simple switching between predefined beams to optimum beam forming. It is anticipated that there will be a tremendous increase in traffic for mobile communication systems in the near future. This is because the number of users are going up and also the new high bit rate data services are being introduced to the existing mobile networks. This trend is observed for second generation (2G) systems and will most certainly continue for 3G systems. The increase in traffic will place a demand on both telecommunications equipment suppliers and operators to find more capacity in the networks. As suggested earlier, one of the most promising techniques for increasing the capacity in mobile networks is the use of smart antennas.

The most important feature of a smart antenna system is its ability to cancel co-channel interference. The radiation from cells that use the same set of channel frequencies is likely to cause co-channel interference. Therefore, co-channel interference in the transmitting mode can be reduced substantially by focusing a directive beam in the direction of a desired user, and nulls in the directions of the other receivers. Similarly, in the receiving mode, co-channel interference can be reduced by knowing the directional location of the signal's source and utilizing interference cancellation.

For a smart antenna system to function properly, it needs to differentiate the desired signal from the co-channel interference, and normally this requires either "a priori" knowledge of a reference signal, or the direction of the desired signal source, in order to achieve its desired objectives. There are various methods in literature to estimate the direction of sources with conflicting demands of accuracy and processing power. Also, there exist a variety of algorithms with various speeds of convergence and required processing time to update array weights. In some applications the properties of signals can be exploited, eliminating the need for training signals[1,36].

This chapter will present and analyze the recent research on the advances of the smart antenna technology and their applications in mobile communications.

3.2 Beamforming Algorithms

Various smart antenna or beamforming algorithms and their implementations in simulation environments have been reported in the past [2,6,7,28]. Two main adaptive techniques have been adapted to find the optimal weight vector: training based techniques and blind techniques. In the training based schemes, a desired signal must be supplied using either a training sequence or overlay pilot. The blind adaptive algorithms, on the other hand, does not need training sequences. Several adaptive algorithms, which adapt these two techniques, will be discussed in this Chapter.

The first beamforming algorithm is based on the Least Mean Squares (LMS) principle and was proposed nearly 40 years ago in [7]. This is a training based method and therefore a pilot symbol is required in the adaptation process. Though the convergence can be slow, the simulation results are shown to be in good agreement with the theory.

In [2], an adaptive algorithm based on Least Squares method is developed for CDMA systems: known as LS-DRMTA (Least Squares De-spread Re-spread Multi Target Array), it makes use of the properties of CDMA (spreading modulation and PN sequences) to efficiently estimate the weight vectors. The implementation of this algorithm will be discussed in Chapter 5.4.2.

The LS-DRMTA utilizes the spreading information of each user, which is a key factor in CDMA in distinguishing different users occupying the same frequency band. Furthermore, this technique has several advantages over the other algorithms [2].

- Since each user has a different spreading sequence, the weight vector of each different user is updated with a different tendency and thus the optimum weight vectors will be different for each user.

- Since different weight vectors are adapted with different PN sequences, the weight vector adapted by using the i^{th} user's spreading signal will correspond to the i^{th} user. Therefore, there is no need to perform the sorting procedure.

- The number of antenna elements in the array does not limit the number of output ports of the beam former.

- The computational complexity of the LS-DRMTA is lower than that of other multi target adaptive algorithms.

The above LS-DRMTA will be applied to WCDMA in this thesis.

CMA (constant modulus algorithm), introduced by Godard, is a blind adaptive algorithm received recent attention in mobile communications. This can be applied to signals transmitted with constant envelopes. A CMA based adaptive array will attempt to drive the signal at the array output by exploiting the low modulation variation of the communication signal (e.g, PSK, FSK and QAM)[38]. It also showed in [38] that CMA performs well in reducing narrow band fading conditions and CMA may be easily applied to analog frequency-modulated signals. However there are several drawbacks to this approach. For instance, CMA my capture the strongest constant envelope signal irrespective of whether the captured signal is an interfering signal or the desired signal. Furthermore this approach is not as well-characterized as that of MMSE and LS. To address this interference capture problem, a multi-target CMA has been developed by Agee [40]. This approach is known as LS-CMA (Least Squares Constant Modulus Algorithm) and it uses an extension of the method of nonlinear least squares.

There are several other blind adaptive algorithms which function by restoring spectral coherence (a property of most communication signals). One such algorithm known as SCORE (Self Coherence Restoral), which exploits cyclostationarity of communication signals, has been presented in [39]. Cyclostationarity of signals simply means that the signals are correlated with frequency-shifted version of themselves. The SCORE approach has several drawbacks, such as very slow convergence, very high complexity, and vulnerability: immune to capture problem at instances where spectrally self-coherent interferences are present at the reference frequency. Another cyclostationarity based technique is the SLA (Spectral Line Approximation) reported in [40]. SLA is a much improved approach which is less vulnerable to interference and is computationally simpler compared to SCORE approach. However, SLA still has the capture problem.

Recently, some blind beamforming algorithms have been proposed for CDMA applications [10-13]. The common approach in these algorithms is to use the MSINR (Maximum Signal to Interference and Noise Ratio) criteria to form the beams in the spatial domain. Various techniques can be used in a CDMA environment to maximize the signal to interference and noise ratio (SINR) at the beam-former output. Among these are the Code Filtering Approach (CFA), the modified CFA and the Code Gated Algorithm (CGA) [21]. The basic idea behind these algorithms is to set up a Generalised Eigenvalue (GE) problem and then find the optimum weight vector, which is the principal eigenvector (the eigenvector corresponding to the maximum eigenvalue) of the GE.

In CGA, the statistical properties of the desired signal and the interference plus noise are estimated by exploiting the separation of the desired signal from the interference after de-spreading operation on the received CDMA signal [13]. The signal separation has been implemented using LPF (Low Pass Filters) and High Pass Filters (HPF) to separate the signal component and noise plus interference component. The basic concept of CGA is shown in Fig.3.1 (This CGA has been presented for information only and has not been applied directly in our simulation).

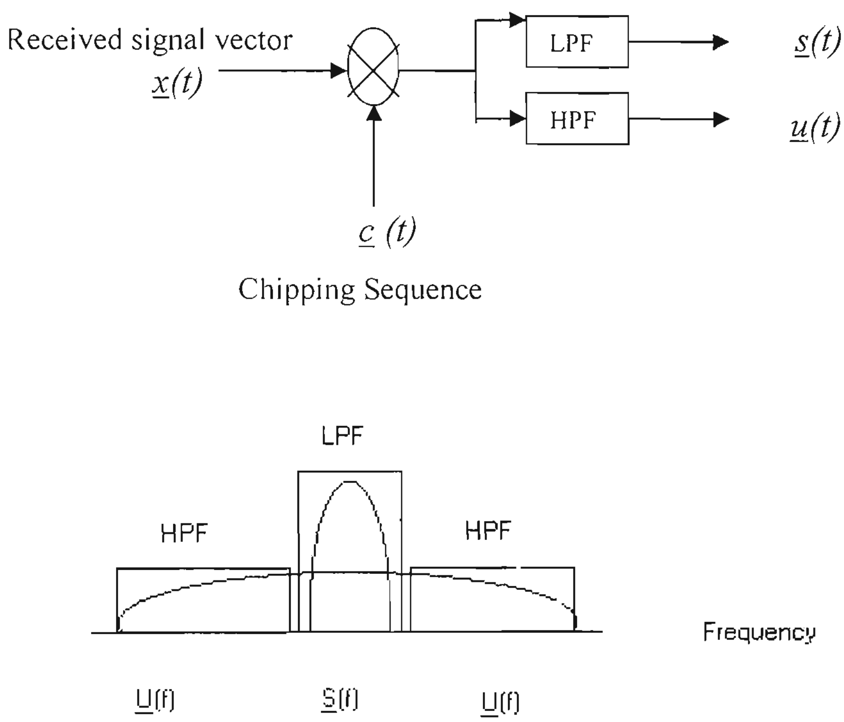

Figure 3.1: The basic concept of CGA.

The received CDMA signal is expressed as follows [13]:

$$\underline{x}(t) = \sqrt{P_1}\, b_1(t-\tau_1) c_c(t-\tau_1) e^{i\phi_1} \underline{a}_1 + \sum_{i=2}^{N} \sqrt{P_i}\, b_i(t-\tau_i) c_i(t-\tau_i) e^{i\phi_i} \underline{a}_i + \underline{n}(t), \quad (3.1)$$

where, $\underline{a}_i$=Spatial signature,

b_i =Data bit,

c_i= Spreading code,

τ_i= Receive time delay,

ϕ_i= Receive phase offset and

P_i= Signal power for i^{th} user

The code-correlated signal is expressed as follows:

$$\underline{x}_1(t) = \underline{x}(t) \times c_1(t)$$

$$= \sqrt{P_1} b_1(t-\tau_1) e^{j\phi_1} \underline{a}_1 + \sum_{i=2}^{N} \sqrt{P_i} b_i(t-\tau_i) c_1(t-\tau_1) c_i(t-\tau_i) e^{j\phi_i} \underline{a}_i + \underline{n}(t) c_1(t-\tau_i) \tag{3.2}$$

Then the low pass filtered signal for the desired user becomes

$$\underline{y}_1(n) = \frac{1}{\sqrt{T_b}} \int_{(n-1)T_b+\tau_1}^{nT_b+\tau_1} \underline{x}_1(t) dt$$
$$= \sqrt{T_b P_1} b_1(n) e^{j\phi_1} \underline{a}_1 + \mathbf{i}_1 + \underline{n}_1 \ . \tag{3.3}$$

To implement the high pass filter operation the following approach has been utilized. The idea is to subtract the low pass filtered signal from the input signal:

$$\underline{u}[n] = \alpha\, \underline{x}_1(n) - \beta\, \underline{y}_1(n). \tag{3.4}$$

Using the above equation the desired signal component can be eradicated by a properly selecting α and β in the equation without changing the interference and noise signal statistics. Hence $\underline{u}(n)$ can be used as a good estimate of only interference and noise.

The CGA is a promising approach though the complexity associated with the implementation can be high.

A similar adaptive algorithm has been implemented in [10] to obtain the optimal weight vector that maximizes the SINR at the output of the array system. In this approach, the total computational load is claimed to be 8.5N (N= No of antenna elements) and also, the performance gain of the antenna array is proved to be substantial compared with single antennas. However, both of these methods have been demonstrated for uniform data rate applications only and hence, not necessarily suitable to be used in WCDMA applications (i.e., mixed rate). Most importantly, it has been suggested in [10] that better performance with less complexity can be achieved by combining the pilot based and blind beam forming algorithms.

In [35], an adaptive antenna array with combined algorithms is examined. Temporal updating algorithms such as LMS (Least Mean Square error) and RLS (Recursive Least-Square) take a long time to converge into the optimum antenna weights as the updating of the antenna weights takes place sample by sample in time domain. In contrast, spatial spectral estimation methods such as DFT (Discrete Fourier Transform), MEM (Maximum Entropy Method) or MUSIC (Multiple Signal Classification) can estimate the direction of arrival (DOA) and SNRs by analyzing the spectrum of arriving signals, which are estimated with spatially sampled signals by each element. Then the optimum weight coefficients can be derived by substituting them into the Wiener solution. The advantage of this type of algorithms is that the optimum weight coefficients can be obtained by one snapshot for the purpose of quick adaptation in a time-varying channel. This proposed hybrid or combined DFT and LMS algorithm takes advantages of both methods such as quick adaptation and less complexity. The implementation procedure of the proposed algorithm is presented as follows:

- Derive and approximate best weight coefficients by estimating DOA with DFT algorithm based on spatially sampled signals by using antenna array.

- The weight coefficients derived by DFT algorithm are set as initial coefficients and weight coefficients are updated by using LMS algorithm.

The results of the proposed method have been presented in terms of the rate of convergence with respect to the number of antenna elements. Further it has been observed that the more antenna elements are used the better the results are.

In summary, the above method using combined DFT and LMS algorithm can improve the performance of both time updating algorithm and spatial estimating algorithm. However, more research is required to examine its performance in mixed data rate applications such as WCDMA for a typical number of antenna elements (4 to 12).

GE (Generalized Eigenvalue) problem is one of the challenges that has to be addressed in the blind beam forming algorithms and several techniques have been suggested in solving the GE in order to form the MSINR beam. The Generalized Power Method is a widely used technique to solve the GE. However, it is computationally complex to implement. Another method is the Generalized Lagrange Multiplier (GLM), that can more easily be used to solve the GE (i.e., the computational loading is linear with the number of antenna elements).

In [21], the Adaptive Matrix Inversion (AMI) scheme was presented for the up link of a WCDMA system in FDD mode and a performance comparison has been carried out against GLM in terms of Bit Error Rate (BER) vs. E_b/N_0. Finally, the results obtained from AMI method showed that the performance gain is better from AMI than from GLM while keeping the computational complexity linear with the number of antenna elements. However, there are few limitations associated with this technique. One is that MSINR beam forming has been carried out on I channel of the signal, although Q channel is specified to be the control channel according to WCDMA specifications. Further, the number of interferers taken into consideration is very small.

A performance comparison is given in [12] between pilot symbol assisted and blind beam former- rake receivers at the up link of 3G CDMA system. The criteria used are the pilot symbol assisted (PSA) Least Mean Square (LMS) technique and the blind Code Gated Algorithm (CGA). The results, obtained for a 4-element antenna, showed that the CGA based receiver outperforms the LMS based receiver. In addition, it implies that pilot based techniques could be further improved for better performance of smart antenna receivers in WCDMA applications. A similar performance enhancement study has been conducted in [8] for adaptive antennas in a micro-cellular network.

As indicated above, a significant amount of research has been carried out in developing and analyzing adaptive beam forming techniques. Nevertheless, further research is required to develop adaptive beam-forming techniques in WCDMA multi-rate applications using Q channel. Hence, it is anticipated that this research will make a useful contribution towards filling such a gap.

Chapter 4

Simulation Models

4.1 Introduction

This chapter outlines the basic components of the simulation model used through out the research to evaluate the proposed solution in terms of Bit Error Rate (BER), radiation plots and pole capacity. BER ratio is calculated as the ratio of error bits to the total number of bits transmitted. The results obtained are given in Chapter 6. The main components of the simulation program are transmitter, receiver and the channel model. The simulation program has been written in the MATLAB environment for up link transmission in FDD (Frequency Division Duplex) mode according to the UTRA-WCDMA (UMTS Terrestrial Radio Access -Wideband Code Division Multiple Access) specifications. A basic block diagram of the simulation model is presented in Fig.4.1.

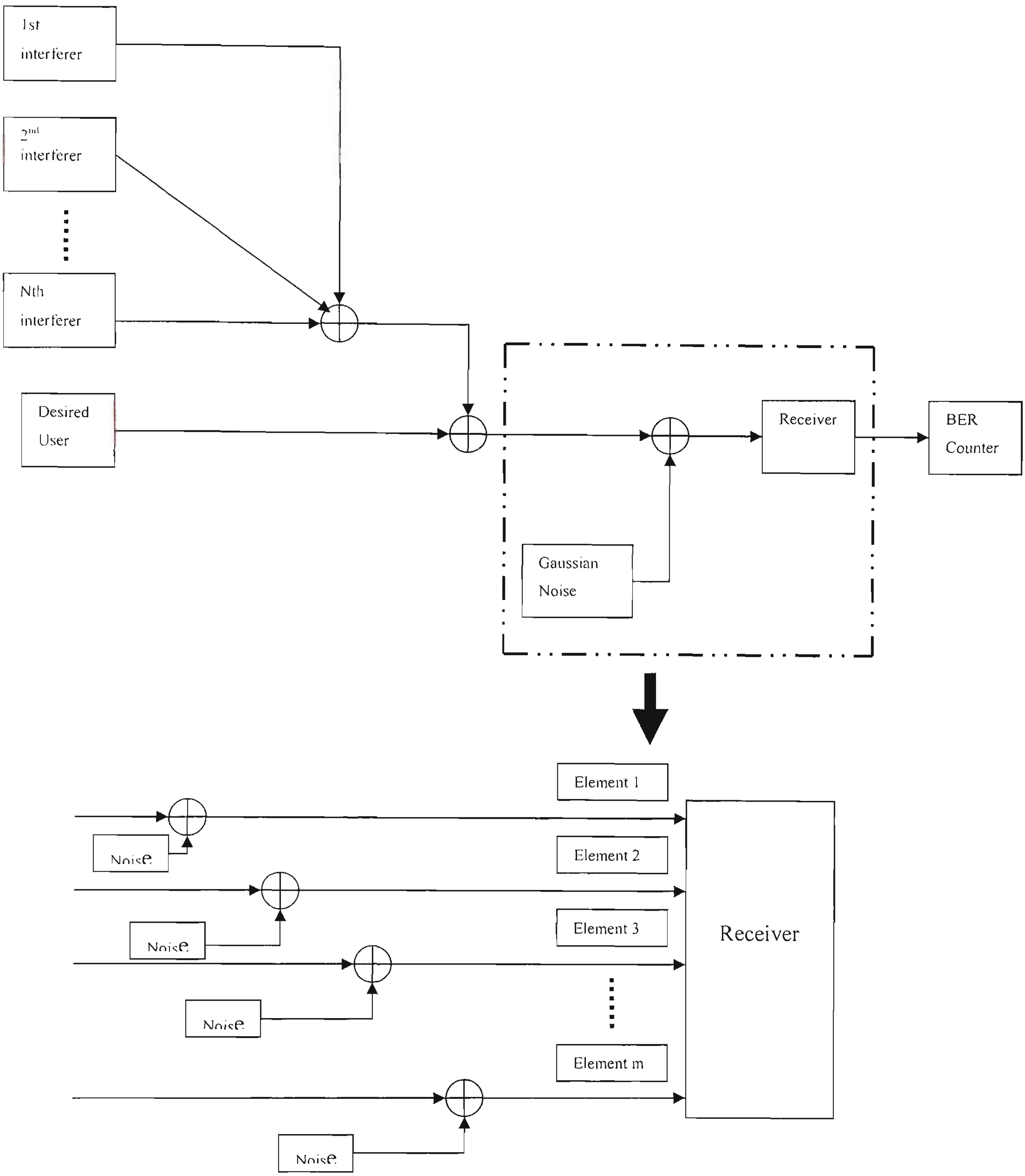

Figure 4.1: Block diagram of the simulator.

4.2 Transmitter Model

The transmitter and the receiver developed for the smart antenna simulation program was constructed using the WCDMA physical layer (as described in Chapter 2). Data are transmitted on a frame by frame basis over a time varying channel. AWGN (additive white Gaussian noise) is added at the front of the receiver. Finally, data are collected at the BER counter.

The basic transmitter model for the simulation is presented in Fig.4.2.

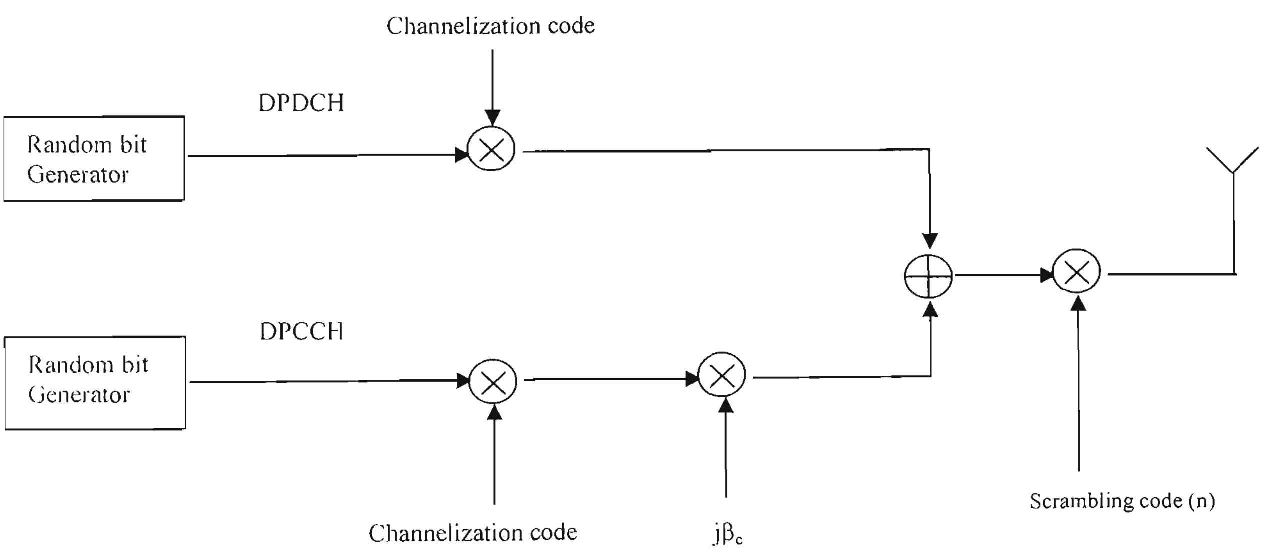

Figure 4.2: The transmitter for the user *n*.

The bits generated by two independent random bit generators are assumed to be the data traffic and control traffic respectively for each user, as is shown in Fig.4.2. The size of the block of bits used for the simulation is one frame, which is

10ms in duration. The channelization codes corresponding to different spreading factors are used to multiply the bits in DPDCH/DPCCH in order to achieve the chip rate of 3.84Mcps. The spreading factor (SF) can vary from 4 to 256 to achieve the corresponding bit rates of 960kbps to 15kbps. The relationship between the spreading factor, the bit rate, information bit rate and the power ratio (β_c) between DPDCH and DPCCH are shown in Table 4.3. The power ratio, β_c, is a parameter that depends on the data rate in DPDCH. The information bit rate depends on both data rate and coding rate.

In our simulation, for uniform data rates we assumed that the bit rate of the desired user in the DPDCH is 60kbps (i.e., SF of the channelisation code = 64) and 15kbps (SF=256) in the DPCCH. In the non-uniform data rate simulations, we introduced a high data user of 960kbps (SF=4) into the uniform data rate scenario.

The next step is to add both data bits and control bits together before the scrambling process. In the scrambling process each user is assigned a unique scrambling code, which is selected randomly from Gold codes in the simulation program.

SF	64	16	8	4
Data bits (kbps)	60	240	480	960
Information bit rate (kbps)	12.2	64	144	384
Power ratio (β_c)	0.5333	0.3334	0.2667	0.2667

Table 4.3: Variable bit rates.

4.3 Channel Models

The discussion in this section is limited to the channel models considered in this thesis. The first part is a brief description of the spatial channel model while the second part gives a detailed description of the Rayleigh fading channel model.

4.3.1 Spatial Channel Models

Smart antennas use spatial properties of the incident signal. Hence classical channel models, which provide only signal power level variations, are not sufficient to analyze smart antenna systems. A more accurate model that incorporates the angle of arrival (AOA) information of the signal is required for the study of antenna arrays. In fact there have been several approaches in the literature that utilize spatial properties of smart antennas. However, we would like to focus our discussion on spatial channel models based on the following equation, as it is of importance in this research [2].

$$\underline{u}(t) = s(t-\tau_0(t))\sum_{i=0}^{L(t)-1}\alpha_i(t)\underline{a}(\phi_i(t))+\underline{n}(t) = s(t-\tau_0(t))\underline{b}(t)+\underline{n}(t), \qquad (4.1)$$

where, $\underline{u}(t)$: Spatial channel output vector,

$s(t)$: Base band complex representation of the transmitted signal,

$L(t)$: No of multi path components,

$\alpha_i(t)$: Complex amplitude of the i^{th} multi path component,

$\tau_i(t)$: Path delay of the i^{th} multi path component $=\tau_0(t)$ for all i,

$\underline{a}(\phi_i(t))$: Steering vector of the antenna array in the direction of arrival $\phi_i(t)$,

$\underline{n}(t)$: Noise at each antenna element, and

$\underline{b}(t)$: the "spatial signature" of the narrow band signal.

4.3.2 Time Varying Channels

This section presents the basics of Rayleigh fading channel and the implementation of Rayleigh fading simulation program.

In a mobile-basestation application, communications between the transmitter and the receiver is mainly achieved by the scattering of the electromagnetic waves as the direct line of sight (LOS) between the transmitter and the receiver is typically blocked by obstacles such as buildings and trees. The electromagnetic propagation by scattering is either by reflection or diffraction from the obstacles. As a result, the received signal at the mobile or base station is a combination of many scattered radio signals. The fluctuations of these signals are characterized by Rayleigh fading. We used Clarke's model for the fading channel simulation.

4.3.2.1 Clarke's Fading Model

Clarke developed a random process model for the received power of random interfering waves [4]. This model has been developed based on the following two assumptions. Firstly, it was assumed that the transmitter is fixed with a vertically polarized antenna. Secondly, the field incident on the mobile antenna is comprised of M equal amplitude azimuth plane waves with arbitrary angles of arrival (AOA) and arbitrary phases.

Each incident wave is associated with a Doppler shift due to the motion of the mobile. The maximum Doppler shift is given by:

$$f_d = \frac{v \cdot f_c}{c}, \qquad (4.2)$$

where, f_d =Maximum Doppler Shift,

v =Velocity of mobile,

c =Velocity of electromagnetic radiation and

f_c =Carrier frequency of scattered wave.

Based on the above assumptions, Clarke derived the power spectral density function $S\ (f)$ of the resultant RF signal due to Doppler fading[4]:

$$S(f) = \frac{1}{\pi f_d \sqrt{1 - \left(\frac{f - f_c}{f_d}\right)^2}} \qquad (4.3)$$

for $\left|f - f_c\right| \leq f_d$ and

$S(f)$ =0 for $\left|f - f_c\right| \geq f_d$.

In our simulation model, we implemented the power spectrum in the baseband so the frequency considered is $f - f_c$, as is shown in Fig.4.4. To handle the infinite spectral density at the passband edges, we truncated the values at those points to a finite value.

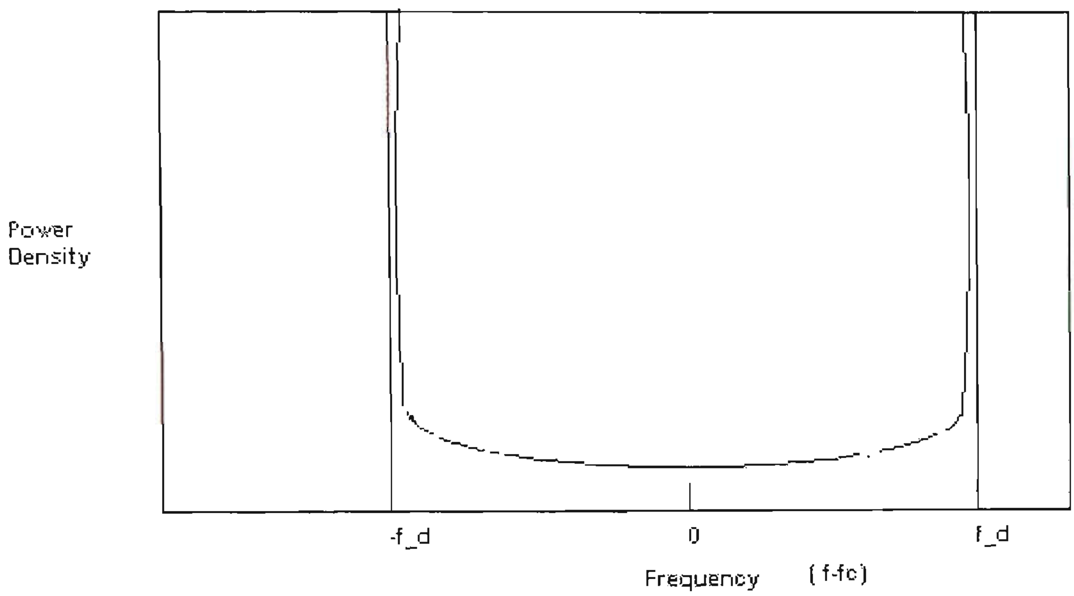

Figure 4.4: Doppler power spectrum implemented at base band.

The following block diagram shows the steps involved in implementing the Rayleigh fading signal.

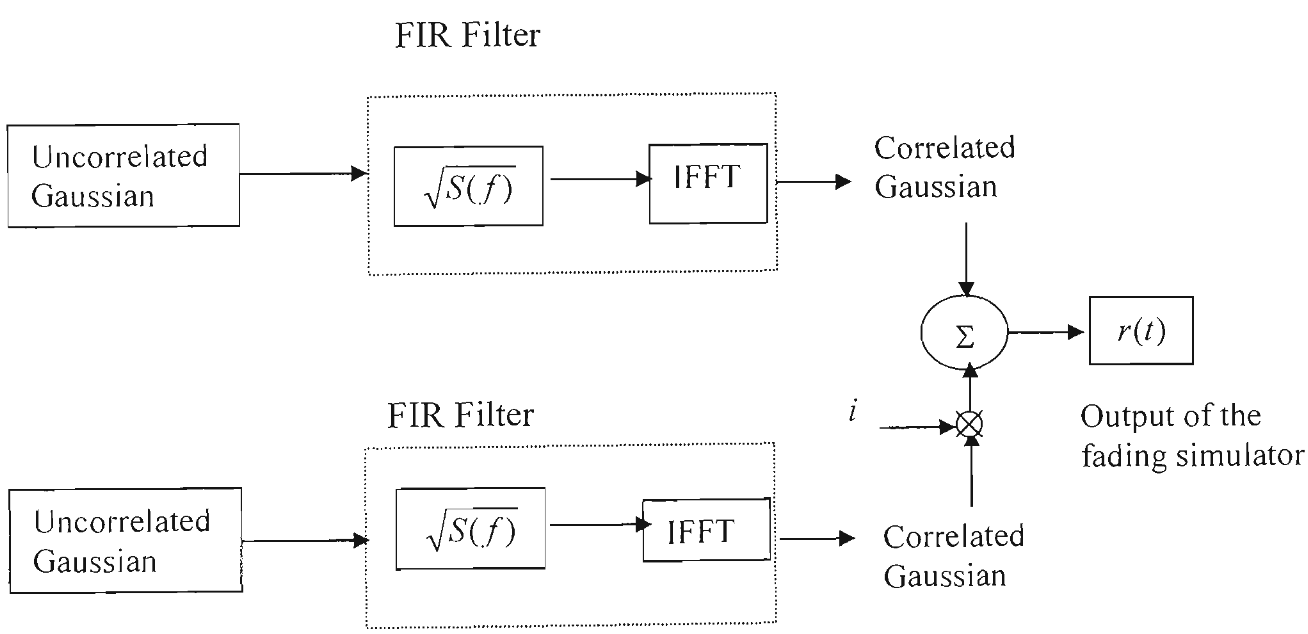

Figure 4.5: Implementation of Rayleigh fading.

In our simulation program, we multiplied the applied signal by the output of the fading simulator $r(t)$ to determine the impact of the fading channel on the applied signal.

The following figure illustrates the signal power level distribution over the implemented Rayleigh fading channel at a carrier frequency of 2GHz and a mobile speed of 2 m/s.

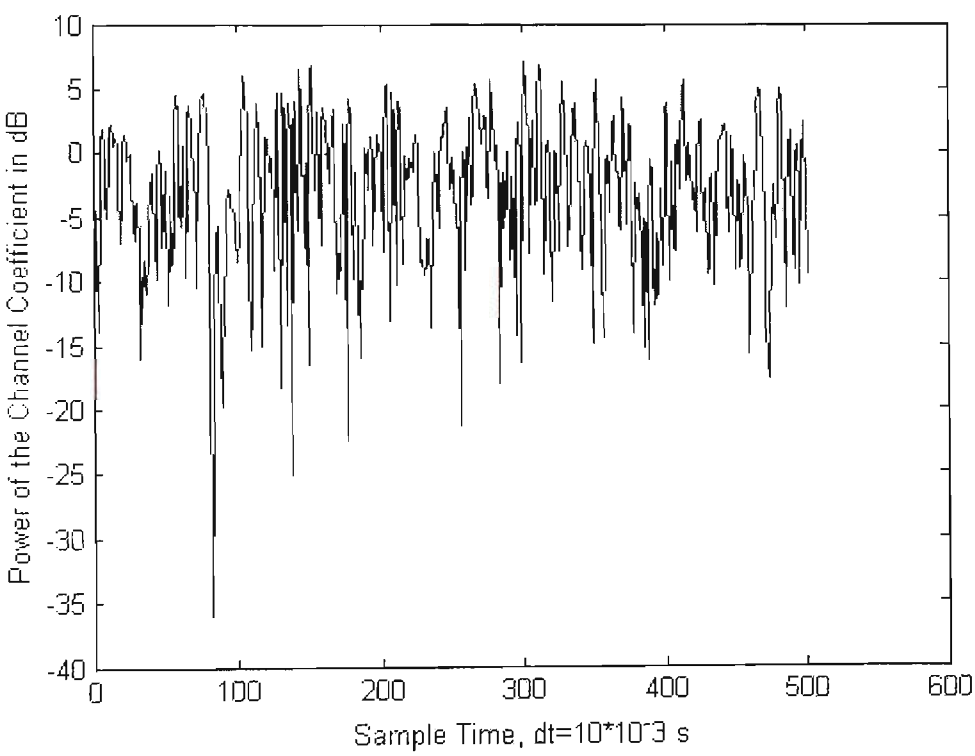

Figure 4.6: Simulated Rayleigh fading envelope at 2GHz.

4.3.3 Channel Simulation Model

In the first stage of the channel simulations, in which the Rayleigh fading is not considered, we used the following simple channel model that was developed from the spatial channel model given in section 4.3.1:

$$\underline{U} = \sum_{i=1}^{N} \alpha_i S_i \underline{a}(\theta_i) + \underline{N}. \tag{4.4}$$

When this model is applied, it was assumed that the transmit-receive system has a perfect power control and no multi path components are associated with the signal of interest. Furthermore, $\underline{N}$, which represents AWG noise, is calculated based on the assumption that SNR=10dB. This evaluation of AWGN using SNR will be given next in section 4.3.3.1. The other parameters in the model are:

$\underline{U}$: Signal received at the base station,

S_I : Signal transmitted by the desired user,

$S_{i\,(2\leq i\leq N)}$: Signals transmitted by the other users (interferers),

$\underline{N}$: Additive White Gaussian Noise (AWGN),

α_i : Fluctuations of amplitude levels of each signal,

m :No of antenna elements (LES (Linear Equally Spaced) array with $\lambda/2$ space),

$\underline{a}(\theta_i)$: Steering vector for the angle of arrival θ_i and,

$$\underline{a}_m(\theta_i) = e^{-j\pi m\cos\theta_i}. \tag{4.5}$$

When m=4, the steering vector is:

$$\underline{a}(\theta_i) = [1, a_1(\theta_i), a_2(\theta_i), a_3(\theta_i)]^T \tag{4.6}$$

4.3.3.1 AWGN

In the channel model simulations, zero mean additive white Gaussian noise (AWGN) is evaluated for a given value of SNR and added in order to introduce the effect of thermal and background noise. In general, SNR is defined as E_b/N_0 in the simulation of digital communication systems, where E_b is the transmit energy per bit and N_0 is the noise power spectral density. In code division multiple access systems, the variance of the noise distribution depends not only on the SNR at the front end of the receiver, but also on the spreading factor (SF), signal amplitude and the sampling rate. The following derivation shows how to find the noise variance for a given value of E_b/N_0 [37].

When chip duration (T_c) and chip amplitude (A) are known, the energy per chip (E_c) can be expressed as

$$E_c = A^2 T_c. \tag{4.7}$$

Then the energy per bit (E_b) is

$$\begin{aligned} E_b &= SF \cdot E_c \\ &= SF \cdot A^2 T_c, \end{aligned} \tag{4.8}$$

where SF is the spreading factor (gain) of the CDMA sequence.

Assuming AWGN channel with two-sided power spectral density of $N_0/2$, the noise variance is given by

$$\sigma^2 = \frac{N_0 f_s}{2}, \tag{4.9}$$

where f_s is the sampling rate.

Therefore, $\frac{E_b}{N_0} = \frac{(SF)A^2T_c}{2\sigma^2 / f_s} = \frac{(SF)A^2(T_c.f_s)}{2\sigma^2}$ (4.10)

Let m denote the number of samples per chip, then

$$m = T_c.f_s, \tag{4.11}$$

From (4.10) and (4.11), the noise variance for a given E_b/N_0 is

$$\sigma^2 = SF(A^2)\frac{m}{2(E_b / N_0)}. \tag{4.12}$$

In the later stage of the simulations, the signals transmitted by the user and the interferers are subjected to Rayleigh fading generated by the time varying channel model that was discussed in section 4.3.2.1.

4.4 Receiver Model

Three antenna structures are considered for simulation in the research. However, only the one antenna structure, namely the omni directional antenna, is discussed in this chapter. The other two, namely the switched beam and the adaptive array antennas, which are deemed as smart antennas, will be described in the next chapter (as the main topic of the thesis). The omni directional antenna is used as a reference for the comparison of the simulation results with switched beam and adaptive array antennas. Throughout the reception process, it is assumed that both channelization codes and scrambling codes are perfectly synchronized with the signal received from the desired user.

The single antenna structure shown in Fig.4.7 (this model may be looked at together with the transmitter model given in Fig. 4.2) was used as the simulation model for the omni directional antenna for WCDMA. The data bits received at the antenna are subjected to de-scrambling and de-channelization and the resulting bits coming out of the receiver are compared with the transmitted data bits of the desired user in order to determine the BER.

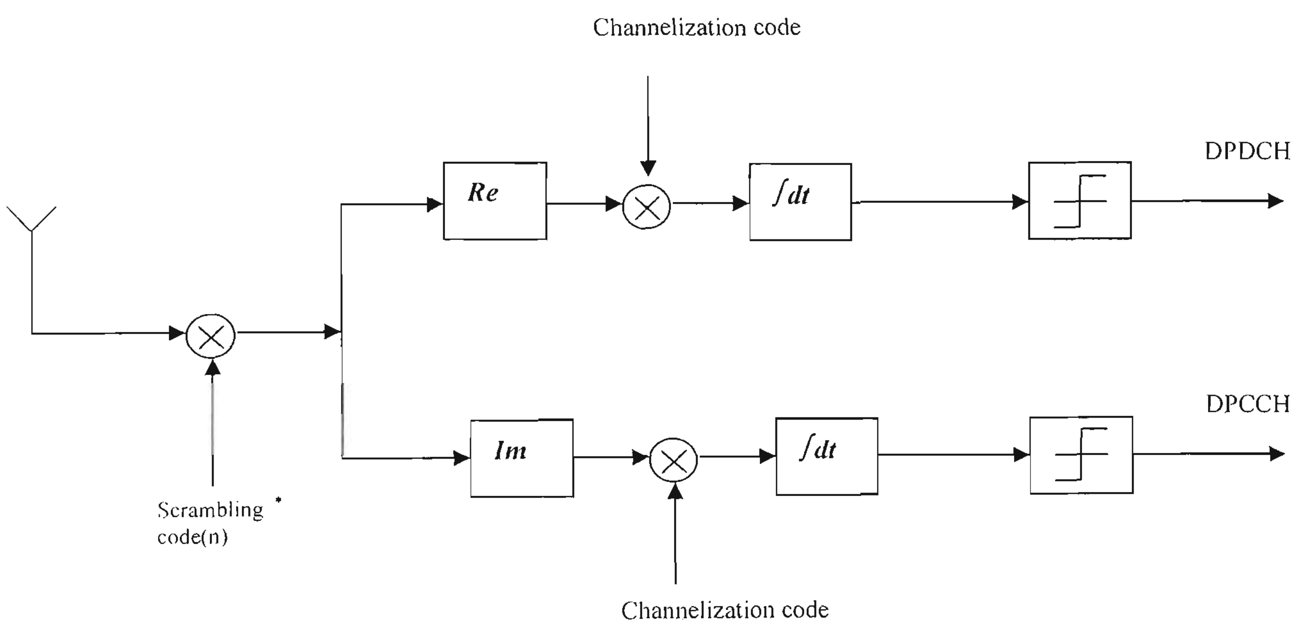

Figure 4.7: The omni directional antenna receiver.

Chapter 5

Smart Antennas

5.1 Introduction

Sectorization of cells is the common technique used in present mobile communication systems to reduce interference and hence to increase capacity. This is achieved by employing dedicated antennas and RF coverage in each sector. The main disadvantage of the current sectorization scheme is that it becomes inefficient with the increase of the number of sectors because of the antenna pattern overlap and the increase in the number of handoffs within the cell.

Smart antennas have been offered as a more efficient technique to reduce interference in mobile communications systems by means of directing narrow beams towards desired user/clusters of users while focusing nulls towards interfering users. This interference reduction means the improvement of the system capacity. Furthermore, as a smart antenna's high directional gain can improve the link budget, an increase in coverage and range can also be expected.

5.2 Antenna Arrays: The Model

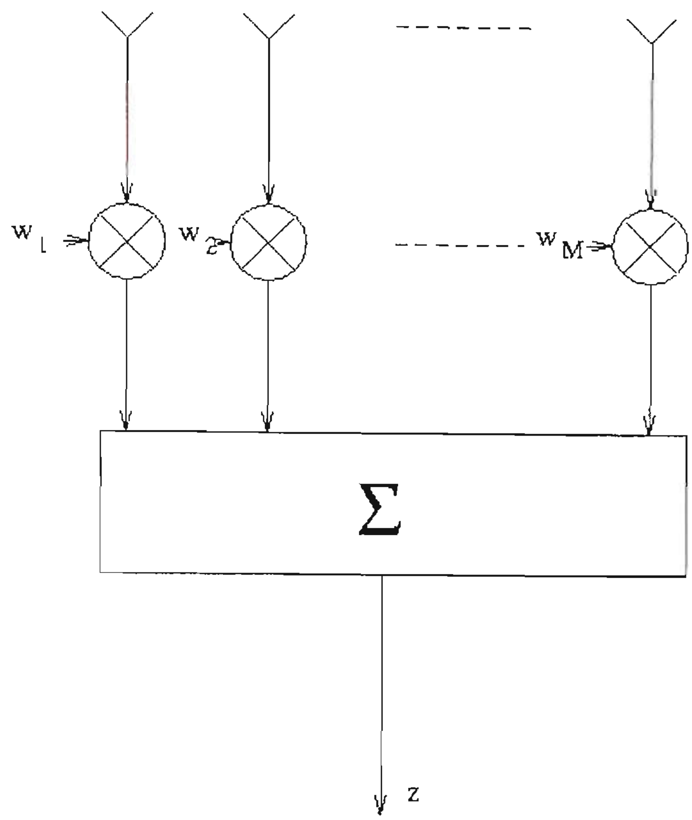

Figure 5.1: A smart antenna system with a linear array.

Smart antenna systems can be defined as a combination of low gain antennas connected by a combining network as is shown in Fig.5.1. Each input signal arriving at the antenna element is weighted by a complex weight denoted by w_1, w_2, ..., w_M. before being demodulated described later in the thesis. As such, the array output, $z(t)$, is:

$$z(t) = \sum_{m=0}^{M-1} w_m u_m(t) = As(t)\sum_{m=0}^{M-1} w_m e^{-j\beta\Delta\varphi_m} = As(t)f(\theta,\phi), \tag{5.1}$$

where w_m : weighting factors,

$u_m(t)$: signal received at the antenna element *m*,

A : arbitrary gain constant,

$s(t)$: the base band complex signal incident on the array,

M : number of elements in the array,

$\beta = 2\pi/\lambda$: propagation factor,

$f(\theta,\phi)$: array factor, and

$$\Delta\varphi_m = \beta(x_m \cos\phi \sin\theta + y_m \sin\phi \sin\theta + z_m \cos\theta).$$

Hence, (x_m, y_m, z_m) is assumed to be the coordinates of the antenna *m*, while θ and ϕ are the elevation angle and the azimuth angle of the incident signal on the antenna element *m* and a reference antenna. For convenience, element 0 is chosen as the reference antenna.

The equation above indicates that we can change the antenna pattern and in particular steer the main beam in a desired direction by adjusting the weights. Since weights are complex numbers, both magnitude and phase variations are possible with each weight.

Smart antenna systems fall into two categories: switched beam arrays and adaptive arrays. A detail discussion of switched beam array and adaptive array antennas are presented in the rest of this Chapter.

5.3 Switched Beam (SB) Array

The switched beam (SB) approach has a relatively low complexity and cost, and it subdivides a typical three macro-sectors further into several micro-sectors. Each micro-sector contains a predefined fixed beam pattern with the highest gain located in the center of the beam and lower elsewhere. During operation the switched beam system determines the best beam pattern (the one that has the strongest signal) from one of the several fixed choices. When the user moves, the system monitors the signal strength and may switch to other fixed beams if necessary.

In comparison to conventional sectored cells, switched beam systems have the potential to increase the range of a base station by anywhere from 20 to 200% depending on the circumstances. This additional coverage can save an operator substantial amount in infrastructure costs and allow them to lower prices for consumers [16,17].

However, there are two significant limitations with switched beam antenna systems. One is due to the signal strength variation as the user moves through the sector. This is because the beams are predetermined and as a mobile user moves toward the far azimuth edges of a beam, the signal strength can degrade rapidly before the user is switched to another micro sector. The other limitation is due to the fact that a switched beam system does not distinguish the difference between a desired signal and interference ones. For instance, if an interfering signal is at the center of a selected beam and the desired user is away from the center of the selected beam, the interfering signal can be enhanced more than the desired signal.

5.3.1 Designing the SB Antenna

The key factor in designing SB antenna systems is to utilize an effective technique for beam selection in a quick and accurate way so that the target subscriber can be covered by selecting the best beam. Fig. 5.2 shows a block diagram of a four-element SB antenna system implemented in our simulations. The basic principle of operation in this simulation program is that it selects the signal of the highest magnitude from the four beam outputs.

Several methods can be used for directing radiated power from an array antenna into a narrow beam. The required phase shift front that corresponds to a narrow beam can be realised either through digital beam forming in the transceivers, or at radio frequency (RF), using passive networks or phase shifters. When RF beam forming is used, the phase coherence can easily be achieved because the phase shift requirements only involve transmission lines within the antenna unit itself. One example of a passive network is the Butler matrix that generates a set of simultaneous orthogonal beams at the RF stage while minimizing the beam-forming loss. Once the beams have been formed, a switch can be employed to select the best beam for the desired user among the finite number of available beams depending on the position of the user.

The switched beam array structure used in our simulations is presented in Fig. 5.2. The weight vectors, $\underline{W}_1$, $\underline{W}_2$, $\underline{W}_3$, $\underline{W}_4$ which are applied before the de-scrambling and de-channelisation process correspond to the coefficients of a 4×4 Butler matrix as shown in equation 5.2. Finally the signal with the maximum magnitude is selected by comparing the power level of each signal at all the 4 output ports. In the demodulation process all the interference signals are filtered out and the signal of interest is passed through.

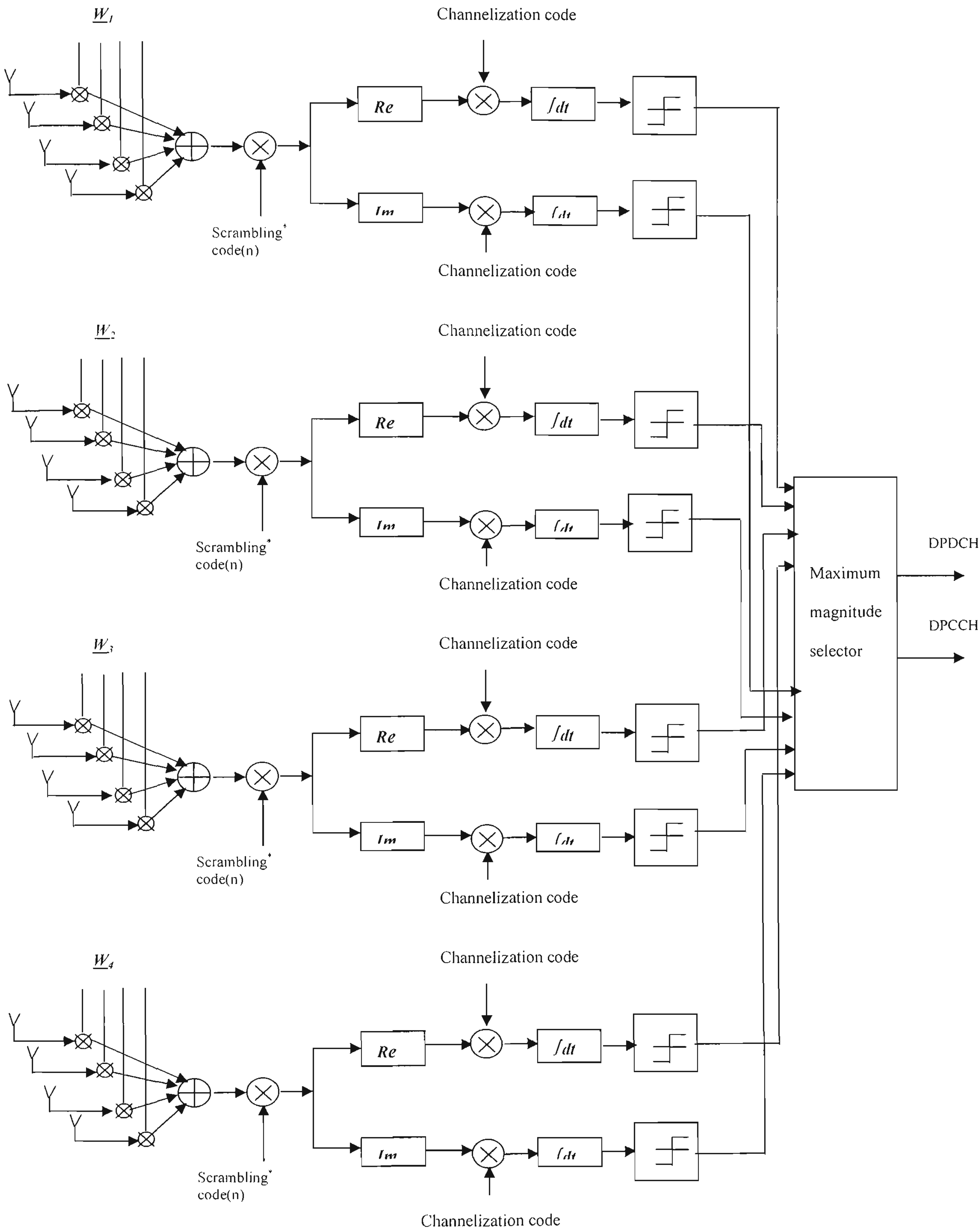

Figure 5.2: The switched beam array receiver.

$$B = \begin{bmatrix} e^{-j\pi/4} & e^{-j\pi} & e^{j\pi/4} & e^{-j\pi/2} \\ 1 & e^{-j\pi/4} & e^{-j\pi/2} & e^{-j3\pi/4} \\ e^{-j3\pi/4} & e^{\frac{-j\pi}{2}} & e^{-j\pi/2} & 1 \\ e^{-j\pi/2} & e^{j\pi/4} & e^{-j\pi} & e^{-j\pi/4} \end{bmatrix} \tag{5.2}$$

5.4 Adaptive Antenna Array

Adaptive antenna arrays are more efficient than switched beam antennas because adaptive algorithms can dynamically adjust the beam pattern to optimize the system performance. To this end, the adaptive algorithms continuously differentiate between the desired signal and multipath and interfering signals according to certain metrics. As a result the beam pattern is continuously updated based on changes in the desired and interfering user locations. This allows the adaptive system to dynamically steer the main beam towards the desired user and nulls towards the interferers.

Adaptive algorithms play a major role in finding the optimum weight vector. Since the mobile environment is time-variable, the weight vector must be updated periodically. At each iteration, the current weight vector ($\underline{w}_i$) is updated using the most recently available data.

Several adaptive algorithms have been widely used and these include Stochastic Gradient technique, Least Mean Square, Recursive Least Square, and the Bussgang Algorithm. More accurate ones are normally mathematically cumbersome to implement because the higher the number of assumptions in the model the harder it becomes to implement. In this research, we will look at a Least Square method and a Lagrange Multiplier method especially developed for CDMA.

5.4.1. History of Adaptive Algorithms

The primary purpose of an adaptive algorithm is to find a set of weights that will allow the output response of the antenna array at each instant of time to be equal or as close as possible to the desired response in an adaptive fashion. It was believed that the first adaptive algorithm criteria was proposed by Wiener nearly 40 years ago. Since then, many adaptive antenna algorithms have been developed by utilizing both space and time based approaches. Some of the work done earlier has been presented in Fig. 5.3 and Eq. 5.3 to 5.12 for the completeness of thesis and has not been applied directly in our simulations.

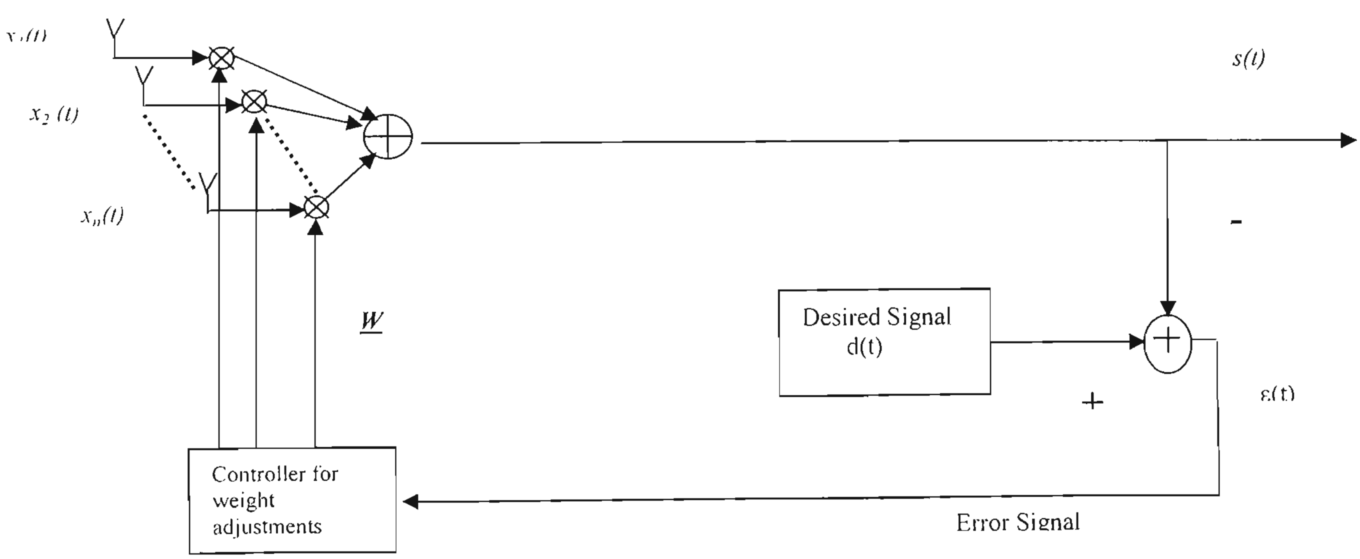

Figure 5.3: The basic adaptive process.

As shown in Fig. 5.3, the input signals **X**(t)=[$x_1(t)$, $x_2(t)$.......$x_n(t)$] are applied to the weights to produce the weighted sum $s(t)$.

Therefore,

$$s(t)=\sum_{i=1}^{n}x_i(t)w_i=\mathbf{W}^T\mathbf{X}(t), \tag{5.3}$$

Where $\mathbf{W}^T$ is the transpose of the weight vector and $\mathbf{X}^T$ is the input signal vector.

In discrete form the output is given by

$$s(j)=\mathbf{W}^T\mathbf{X}(j), \tag{5.4}$$

where the index j indicates the jth sampling instant and **X**(j)=[$x_1(j)$, $x_2(j)$.......$x_n(j)$].

In Fig.5.3, the error signal is given by,

$$\varepsilon(j)=d(j)-\mathbf{W}^T\mathbf{X}(j), \tag{5.5}$$

To find a set of weights **W**, the sum of the squares of the error should be minimized:

$$\mathbf{W}=\arg\left[\min\sum_{i=1}^{N}\varepsilon^2(j)\right]. \tag{5.6}$$

Assuming the input signals are stationary stochastic variables, we can always find a set of weights that minimizes the above mean-square error.

Squaring both sides of equation (5.5) leads to,

$$\varepsilon^2(j) = d^2(j) + \mathbf{W}^T\mathbf{X}(j)\mathbf{X}(j)^T\mathbf{W} - 2d(j)\mathbf{W}^T\mathbf{X}(j) \ . \tag{5.7}$$

We can then take the expected value of both sides of equation (5.8):

$$\begin{aligned} \mathrm{E}[\varepsilon^2(j) &= d^2(j) + \mathbf{W}^T\mathbf{X}(j)\mathbf{X}(j)^T\mathbf{W} - 2d(j)\mathbf{W}^T\mathbf{X}(j)] \\ &= \mathrm{E}[d^2] + \mathbf{W}^T\varphi(x,x)\mathbf{W} - 2\mathbf{W}^T\varphi(x,d). \end{aligned} \tag{5.8}$$

where $\varphi(x,x)$ and $\varphi(x,d)$ are :

$$\varphi(x,x) \stackrel{\Delta}{=} E[\mathbf{X}(j)\mathbf{X}(j)^T] \stackrel{\Delta}{=} \mathrm{E}\begin{bmatrix} x_1x_1 & x_1x_2 & . & x_1x_n \\ x_2x_1 & . & . & x_2x_n \\ . & . & . & . \\ x_nx_1 & . & . & x_nx_n \end{bmatrix}. \tag{5.9}$$

$$\varphi(x,d) \stackrel{\Delta}{=} \mathrm{E}[\mathbf{X}(j)d(j)] \stackrel{\Delta}{=} \mathrm{E}\begin{bmatrix} x_1d \\ x_2d \\ . \\ . \\ x_nd \end{bmatrix}. \tag{5.10}$$

(In equation (5.9) and (5.10), we have dropped the time index j for simplicity). Clearly, $\varphi(x,x)$ is a symmetric matrix of cross correlations and auto correlations of the input signals to the adaptive array. $\varphi(x,d)$ is a column matrix of cross correlations between n input signals and desired response signal.

Differentiating equation (5.8) with respect to **W**, we have the gradient

$$\nabla E\left[\varepsilon^2\right] = 2\phi(x,x)\mathbf{W} - 2\boldsymbol{\varphi}(x,d) \quad . \tag{5.11}$$

To find the optimum values, the gradient in equation (5.11) should be zero. Hence

$\boldsymbol{\varphi}(x,x)\mathbf{W}_{LMS} = \boldsymbol{\varphi}(x,d)$, which immediately leads to

$$\mathbf{W}_{LMS} = \boldsymbol{\varphi}^{-1}(x,x)\boldsymbol{\varphi}(x,d), \tag{5.12}$$

where $\mathbf{W}_{LMS}$ is the optimum weight vector that gives the least mean-square error. Equation (5.13) is known as the Wiener-Hopf equation and it is one of the principal equations in the adaptive antenna technology.

To simplify the computational difficulties in solving the above equation, several methods have been proposed in the literature. For example, two methods were suggested in [7]. One method is based on the gradient search technique and the other is based on a relaxation technique.

5.4.2 Least Squares De-spread Re-spread Multi-target Array (LS-DRMTA)

The LS-DRMTA [2] is efficient and easy to implement, and is one of the main algorithms considered in this research. It is a Least Square method especially developed for CDMA, and therefore makes use of the properties of CDMA (spreading modulation and PN sequences) to efficiently estimate the weight vectors.

As was mentioned before, the LS-DRMTA utilizes the spreading information of each user, which is a key factor in CDMA in distinguishing between different users occupying the same frequency band. Further more, this technique has several advantages over other algorithms (see section 3.2).

The derivation as well as a detailed description of LS-DRMTA is given in [2]. Nevertheless, the basic steps involved in finding the optimum weight vector using LS-DRMTA are given below.

Considering the algorithm in Fig. 5.4 the cost function is:

$$J(\underline{w}_i) = \sum_{k=1}^{K} \left| \underline{z}_k^i - \underline{r}_k^i \right|^2 . \tag{5.13}$$

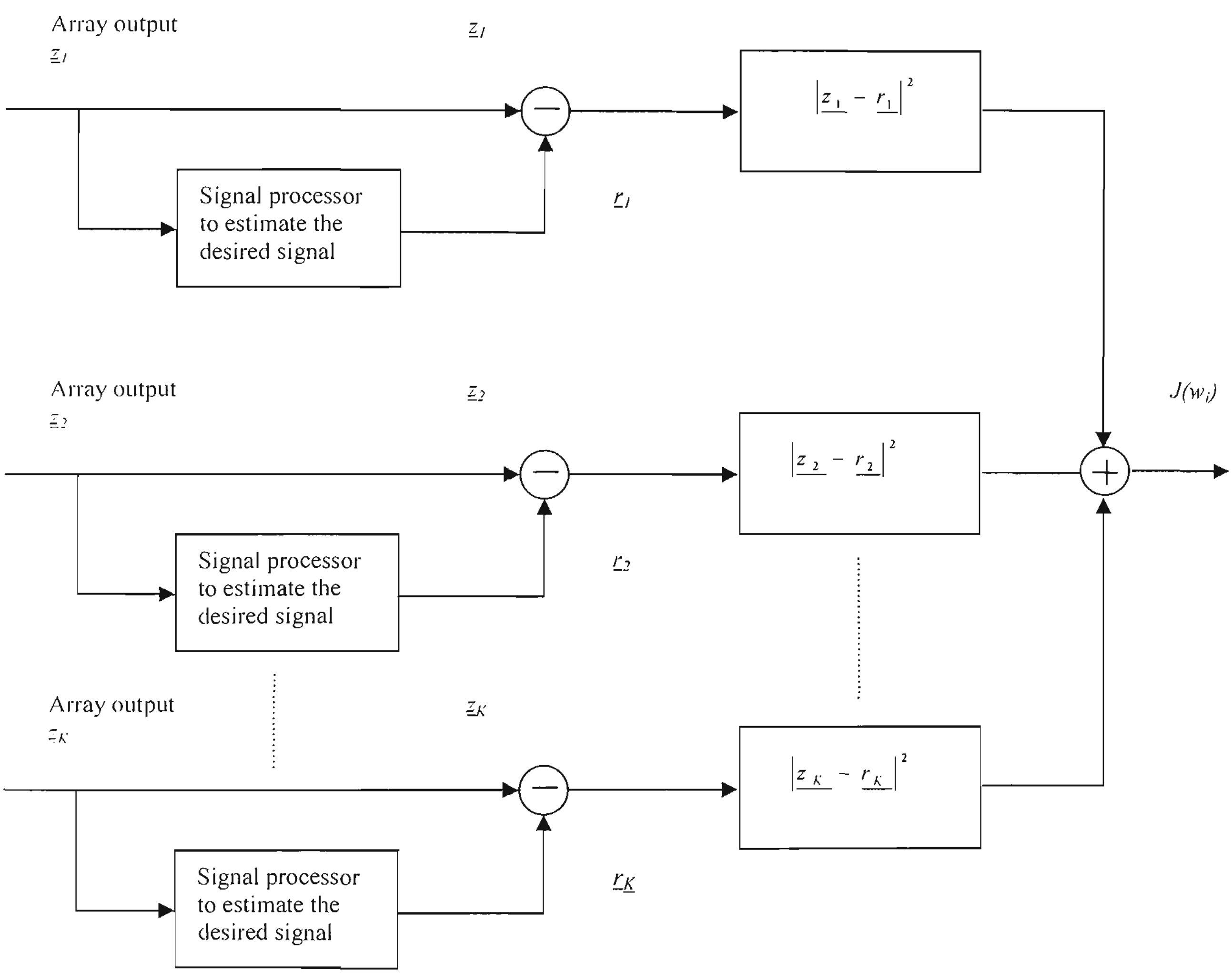

Figure 5.4: The block diagram for $J(w_i)$.

In the above equation,

$\underline{z}_k^i$: the output of the array corresponding to user i, (it is correlated with the time delayed spreading code of the i^{th} user),

$\underline{r}_k^i$: the estimate of the transmitted signal (obtained by re-spreading the received signal using the same spreading code as user i), and

K: size of the data block (This is usually assumed to be the number of samples in one bit period).

Then the weight vector for the user i at the data block index l can be calculated through the following steps:

$$\underline{z}_l^i = (\underline{w}_l^{iH} \underline{U}_l)^T = (z_{(1+(l-1)K)}^i \; z_{(2+(l-1)K)}^i \ldots z_{(K+(l-1)K)}^i)^T \tag{5.14}$$

$$\underline{r}_l^i = (r_{1+(l-1)K-k_{\tau_i}}^i \; r_{2+(l-1)k-k_{\tau_i}}^i \ldots r_{K+(l-1)K-k_{\tau_i}}^i)^T \tag{5.15}$$

$$\underline{w}_{l+1} = \left[\underline{U}_l \underline{U}_l^H\right]^{-1} \underline{U}_l \underline{r}_l^{i*}, \tag{5.16}$$

where $\underline{U}_l$ comprises of different data blocks from the received signal.

The step by step implementation of LS-DRMTA algorithm can be summarized as follows[2]:

1. Initialise the p weight vectors $w_1, w_2 \ldots . w_p$ as $p \times 1$ column vectors with the first element equal to 1 and other elements equal to 0.

2. Calculate the array output using the following equation:

$$\underline{z}_i(l) = \left[\underline{w}_i^H(l)\underline{U}(l)\right]^T$$

$\underline{z}_i(l)$: Output data vector of user i over one bit period corresponding to the weight vector w_i in the l^{th} iteration.

$\underline{U}(l)$: Input data vector of K samples in the l^{th} iteration

3. De-spread the i^{th} user's signal using spreading and scrambling codes of user i and estimate the resulting data bit.

4. Re-spread the estimate data bit using spreading and scrambling codes of user i to get an estimate of the signal waveform of user i.

5. Adapt the weight vector w_i of user i using the following equation:

$$\underline{W}_i^H = (\underline{U}\,\underline{U}^H)^{-1}\underline{U}\,\underline{r}^*.$$

$\underline{r}^*$: complex conjugate of r

6. Repeat steps 2 through 5 until the algorithm converges.

7. Take the final weight vector w_i as the optimum weight vector.

The implementation and a technique to estimate the desired signal are presented on page 58 & 59.

5.4.3. Adaptive Antenna Array with I and Q Signals

In our simulation, the adaptive array receiver was realised as shown in Fig.5.5 using LS-DRMTA algorithm. The principle of this algorithm is to minimize the difference between the received signal and a reconstruction of the estimate of the signal transmitted by the desired user. This procedure is known as decision directed (DD) adaptation. The de-spreading and de-scrambling processes in this structure are similar to the other models discussed in the previous section except for the fact that both I and Q signal information is used as an estimate of the signal transmitted by the desired user. Before the minimization process starts, K samples (K=256) are collected as a batch from the received data stream.

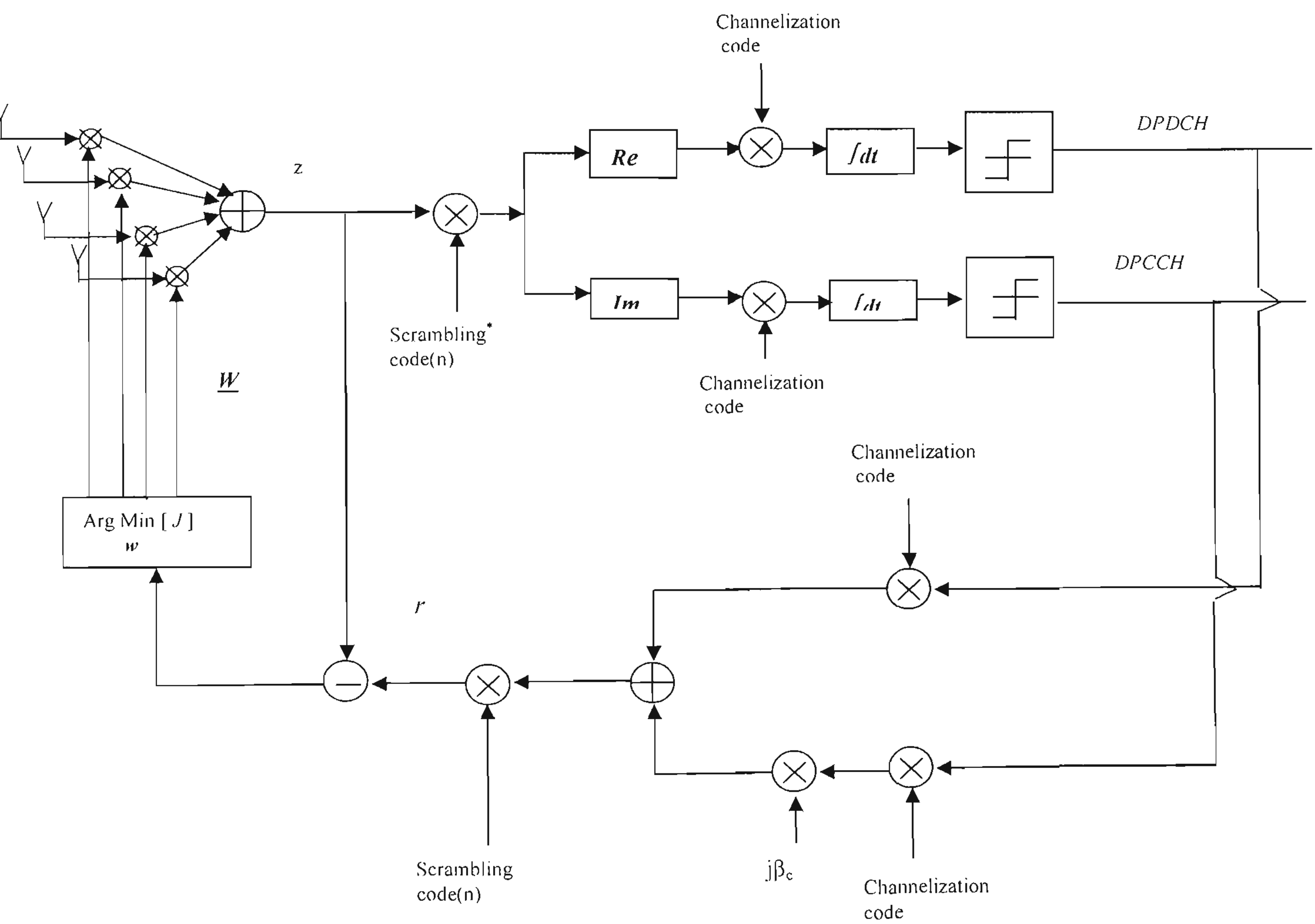

Figure 5.5: Adaptive array receiver.

The following cost function (least squares algorithm in equation (5.13)), was used in the minimization process of our simulations:

$$J(\underline{w}) = \|\underline{z} - \underline{r}\|^2 \tag{5.17}$$

$\underline{z}$ and $\underline{r}$ are vectors of K samples as shown in Fig. 5.5 and then $\underline{z}$ can be expressed as:

$$\underline{z} = \underline{wU} \tag{5.18}$$

New weight vector is calculated in each iteration by solution to cost function $J(\underline{w})$ as shown in equation (5.16):

$$\underline{w}^H = \left(\underline{U}\,\underline{U}^H\right)^{-1}\underline{U}\,\underline{r}^* \tag{5.19}$$

Once the optimum weight vector is found using the Arg Min operation shown in Fig. 5.5, the array output is calculated using the step (2) of the LS-DRMTA implementation algorithm given above. Finally, this array output is subjected to de-scrambling and de-spreading process in order to obtain the DPDCH and DPCCH bits. The obtained results are presented in detail in Chapter 6.

5.4.4. Adaptive Antenna Array with Q Branch Only

To carry out the simulation for the adaptive antenna array with Q branch only, the model given in Fig. 5.5 was modified to accommodate only the Q channel (i.e., with less information). In other words, only Q channel information is used as an estimate of the signal transmitted by the desired user in the de-spreading process of the received signals. The simulation results obtained will be presented in Section 6.3.2.

5.4.5. Lagrange Multiplier (LM) Based Adaptive Algorithm

This is the second algorithm considered in this research. The primary purpose of the adaptive algorithm is to find the optimum weight vector at each snap shot of the received signal. As each subscriber moves, the received signal at the base station receiver varies and each snapshot of signal becomes time dependant.

The derivation of the weight vector in LM is based on the assumption that the eigenvector corresponding to the largest eigenvalue of the auto co-variance matrix of the received signal is approximately equal to the steering vector of the desired signal [33]. For this to be true, the desired signal should be sufficiently larger than each of the interferers at the receiver. As such, the problem of finding the desired beam pattern turns into a problem of finding the eigenvector corresponding to the largest eigenvalue of the auto co-variance matrix of the received signal. There have been several adaptive techniques to find the eigenvector corresponding to the largest eigenvalue. In recent literature, three methods have been listed [32], and they are modified conjugate-gradient method, Lagrange's Multiplier (LM) method and linearized power method. We use the LM method in the simulations in order to find the weight vector.

As mentioned before this algorithm can only be used in an environment where desired signal is sufficiently larger than the interference signals. In fact this condition is inherently satisfied in a normal CDMA system as the desired signal of such a system is larger than the interference signals by the amount of the processing gain of the CDMA system.

Fig. 5.6 shows the adaptive antenna receiver utilized in our simulation. Firstly, the received signal vector $\underline{x}$ is obtained at the output ports of the de-spreader. Then the autocovariance matrix ($\underline{R}_{xx}$) of the received signals is calculated. The vector $\underline{x}$ = $[x_1, x_2, \ldots x_N]$ is a $[N \times 1]$ vector and $\underline{R}_{xx}$ is a $[N \times N]$ matrix, where N is the number of antenna elements.

According to the Lagrange Multiplier (LM) method, the optimum weight vector is determined by the following [33].

$$f(\underline{w}, \gamma) = \underline{w}^H \underline{R}_{xx} \underline{w} + \gamma(1 - \underline{w}^H \underline{w}) . \tag{5.20}$$

where $\underline{w}$ is $[N \times 1]$ weight vector to be computed, γ is the Lagrange multiplier and superscript H denotes the Hermitian operator.

The weight vector at each iteration is found by maximizing the equation (5.17). The weight vector update equation is given by the following equation [33]:

$$\underline{w}(k+1) = \{[1 - \mu\gamma(k)]\underline{I} + \mu \underline{R}_{xx}(k)\}\underline{w}(k) , \tag{5.21}$$

where k is the index at each iteration; $\underline{I}$ is the identity matrix; and μ is the convergence factor.

In the simulation, the following approach is followed for computing the weight vector utilizing the LM based adaptive algorithm[33].

1. Initialize the weight vector $\underline{w}(0)$; we set the first element equal to 1 and the other elements equal to zeros in the initialization vector.

2. New signal vector $\underline{x}$ is obtained at the output of the de-spreader.

3. Array output is computed by

$$y = \underline{w}^H \underline{x} \tag{5.22}$$

4. Lagrange Multiplier is computed by the following equations:

$$A = \mu \tag{5.23}$$

$$B = \mu|y|^2 + 1 \tag{5.24}$$

$$C = \mu|y|^2 + 2|y|^2 \tag{5.25}$$

$$\gamma = [B - (B^2 - A \times C)^{1/2}] / A \tag{5.26}$$

5. Adapt the weight vector $\underline{w}$ using the following equation (5.18):

$$\underline{w}(k+1) = \{[1 - \mu\gamma(k)]\underline{I} + \mu \underline{R}_{xx}(k)\}\underline{w}(k)$$

6. Repeat steps 2 through 5 until the algorithm converges.

7. Take the final weight vector $\underline{w}$ as the optimum weight vector.

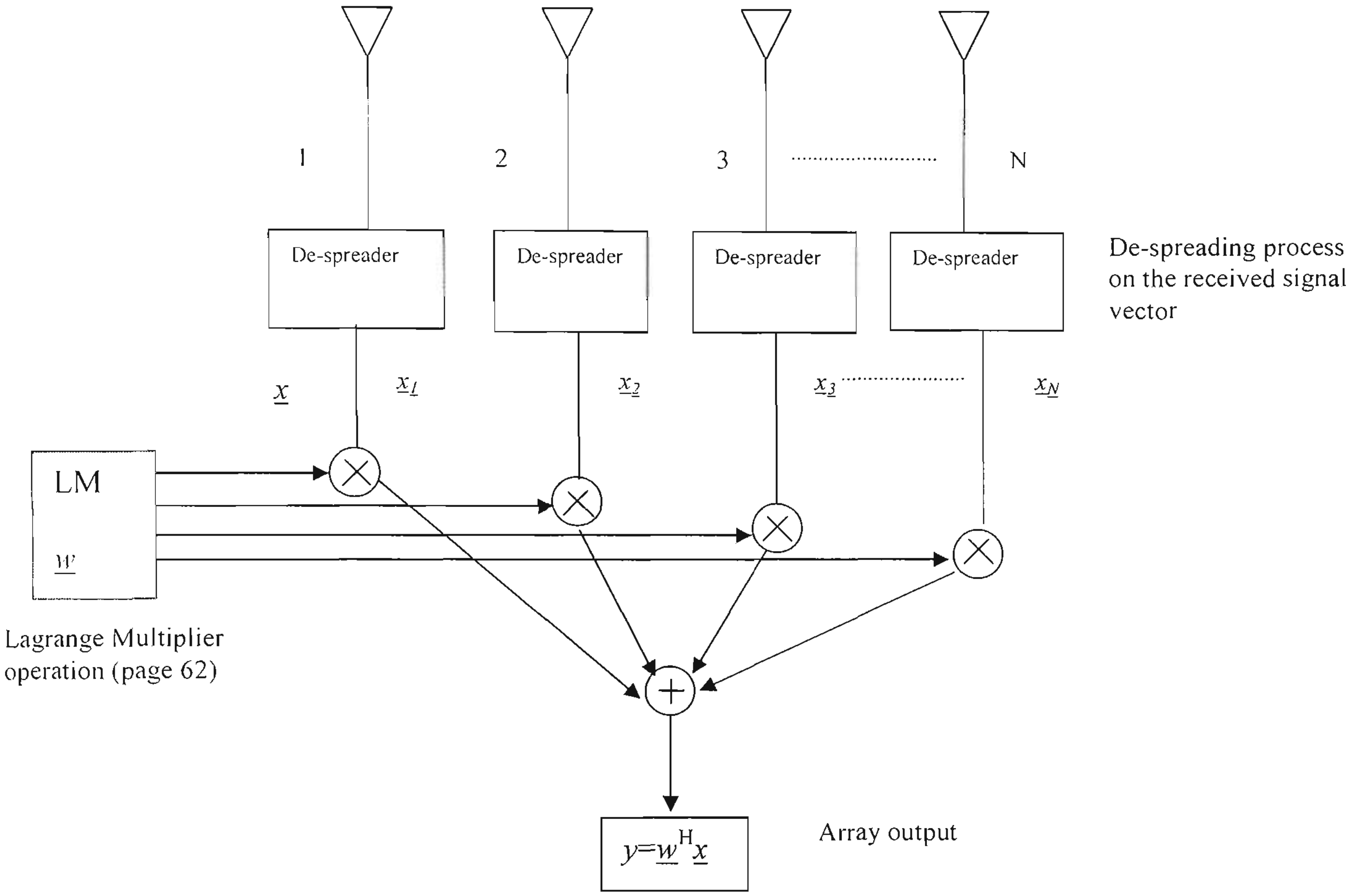

Figure 5.6: The Lagrange Multiplier based adaptive array receiver.

Chapter 6

Performance Comparison Results

6.1 Introduction

This Chapter presents the results of the simulations. The simulation results for mobile users transmitting at uniform data rate (60kbps) are given in Section 6.1. Section 6.2 gives the corresponding BER curves, antenna beam patterns, and pole capacity for the non-uniform data rate scenario with the inclusion of a high data user (960kbps). BER estimate helps to determine the best performing antenna type in terms of a numerical value. Section 6.3 summarizes the results obtained as a result of modification of the simulation program in order to accommodate time varying channel and adaptive algorithm with Q channel only. Finally, section 6.4 presents the BER's of an omni directional antenna system and the LM based adaptive array system in a mixed data rate environment. Also, beam patterns are plotted with respect to different angles of arrival and number of antenna elements in order to obtain a better observation for the adaptation of beam patterns in switched beam and adaptive array antennas.

6.2 Uniform Data Rate Systems

6.2.1 BER

By using the LS-DRMTA algorithm, the BER's for the desired user against the number of interferers were obtained for omni directional, switched beam and adaptive arrays. The input parameters used for the uplink simulation program are listed in Table 6.1.

Desired user = 1, Number of users of uniform data rate = 5-50, Data rate for uniform data rate user = 60kbps, Number of antennas = 4 and 8, Number of simulations = 100, Sector width = 60 / 120 deg, AOA of users = Randomly selected within the above sector width, AOA of the desired user = 90 deg., Number of 10 ms frames = 1, SNR of the desired user = 10dB, Block size for adaptive array = 256, and Values for β used in the simulation = 1, 0.5333, 0.4000, 0.3333, 0.2667 .

Table 6.1: The input parameters used in the simulation.

When the spreading factor is 64 and sector width is 120deg., the bit rate of the desired user is 60kbps (Table 2.4). That means the desired user transmits 600 bits per 10ms frame. The receiving antenna at the other end receives the total of 600 bits transmitted by the transmitter and identifies the number of bits in error. This procedure was then repeated for various number of interferers from 9-59 (i.e., the number of users =desired user + number of interferers), and the obtained BER results are shown in Fig. 6.2.

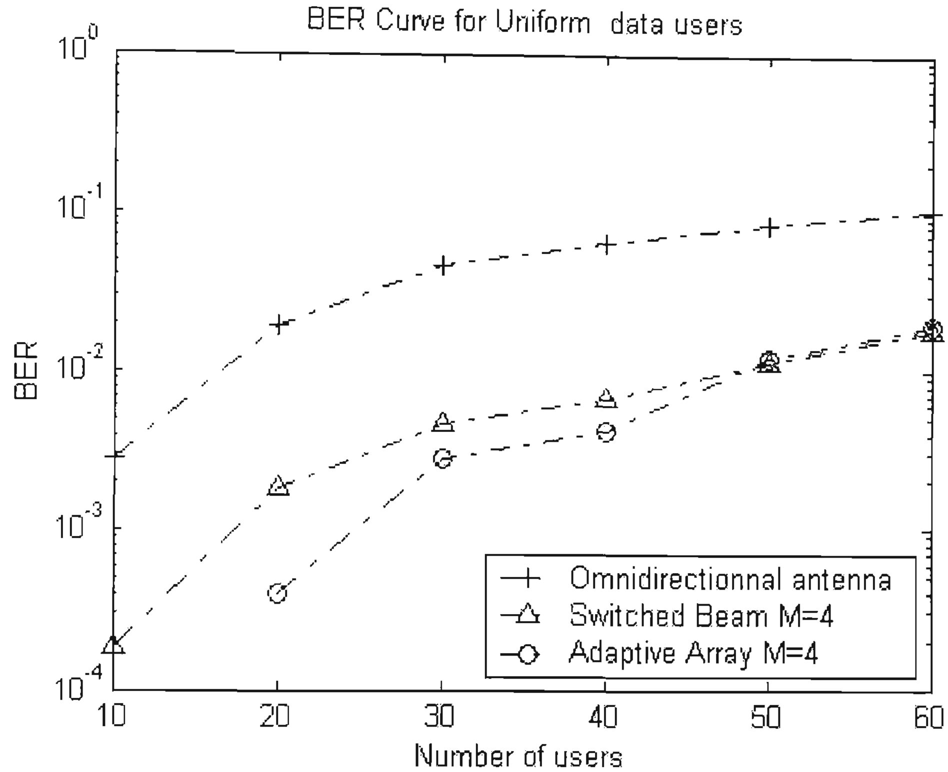

Figure 6.2: The BER for uniform data rate users (4 elements).

We can see from the above figure that the system becomes interference limited as the number of interferers increases. This is predicted with multiple access techniques such as CDMA. Also, the graph shows that BER performance is better for adaptive array system than for omni and switched beam systems. However, the performance gain of the adaptive array over the switched beam array disappears as the number of users approaches 50 (approximately).

The above procedure was repeated for a 60 deg. sector width with all the other parameters remaining the same. The BER's for the desired user vs. number of interferers was obtained and is given in Fig. 6.3 below.

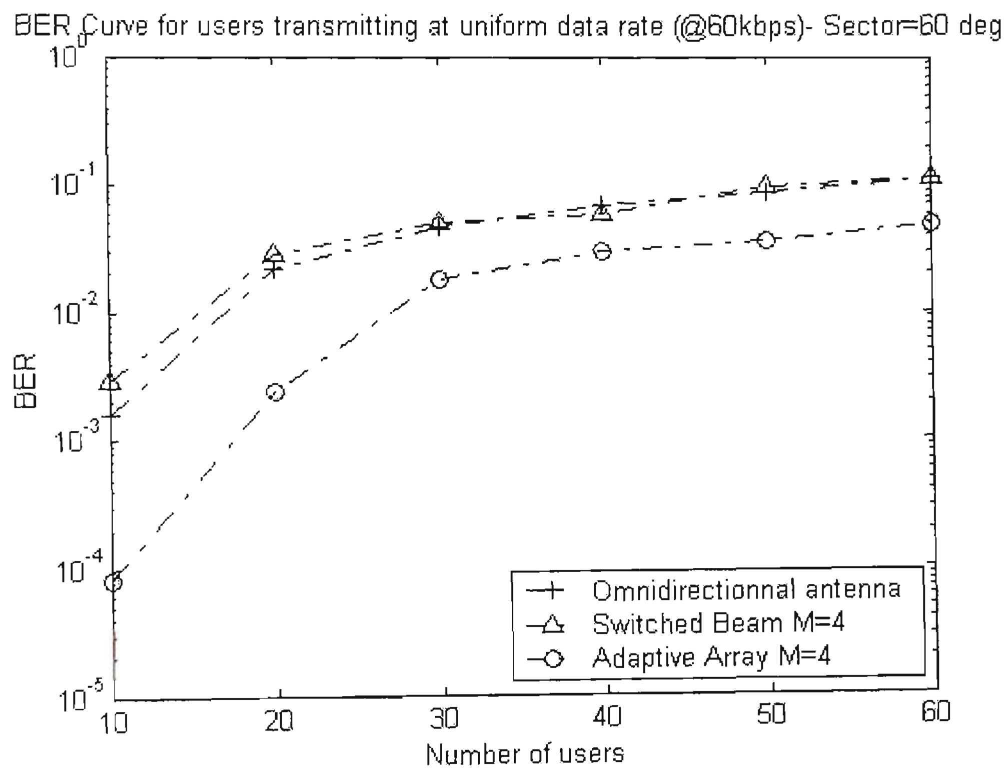

Figure 6.3: The BER's for the sector width of 60 deg.

It can be seen from the two graphs above that BER's of the adaptive array receiver outperforms the switched beam receiver when the sector width decreases. This is due to the capability of the adaptive array system to dynamically steer the antenna beam towards the desired user whereas the switched beam system only has a limited number of fixed beams positions to choose from.

6.2.2 PDF and CDF of BER Results

To plot the PDF (Probability Density Function) and CDF (Cumulative Density Function) curves, the simulation procedure in Section 6.2 was carried out for 200 times when the number of users equals 20. The obtained BER results are presented in PDF and CDF formats in Figs.6.4 and 6.5, respectively. Both plots depict the BER distribution of the adaptive antenna system in comparison with both the switched beam system and the omni directional antenna. These results clearly indicate the potential uplink improvement that an adaptive antenna system can provide over switched beam and omni antennas. It can be noticed from Fig. 6.5 that the BER improvement factor of an adaptive antenna array is approximately 10 times over a switched beam array and approximately 20 times over a single antenna (omni directional antenna).

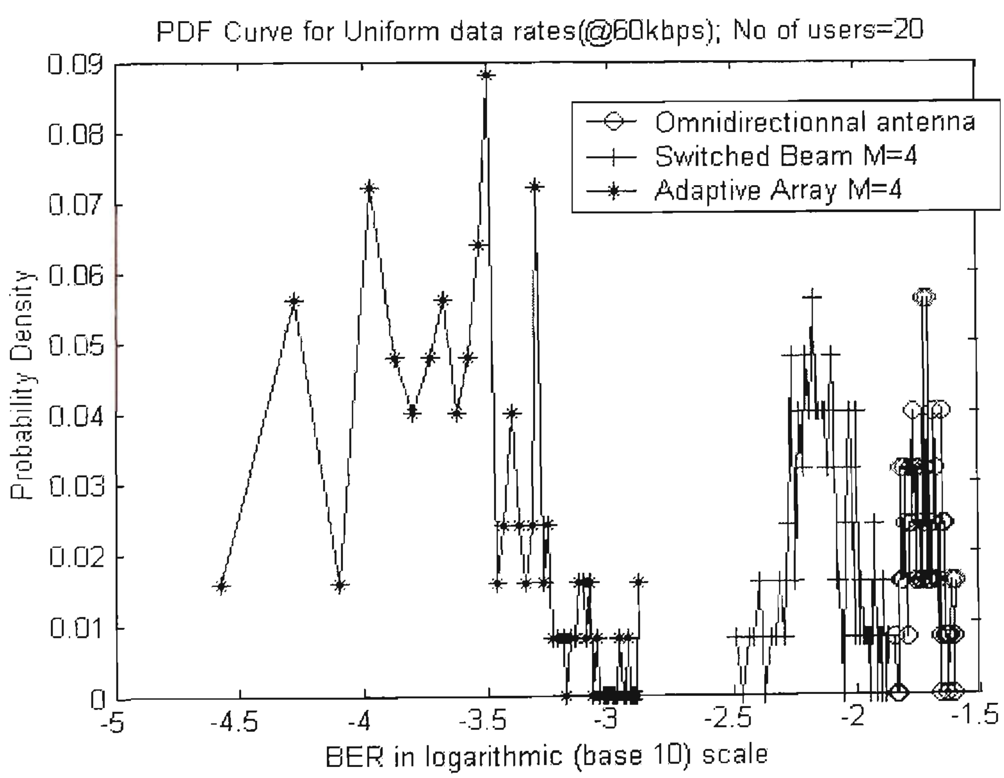

Figure 6.4: The PDF curves for omni directional, switched beam and adaptive array antennas.

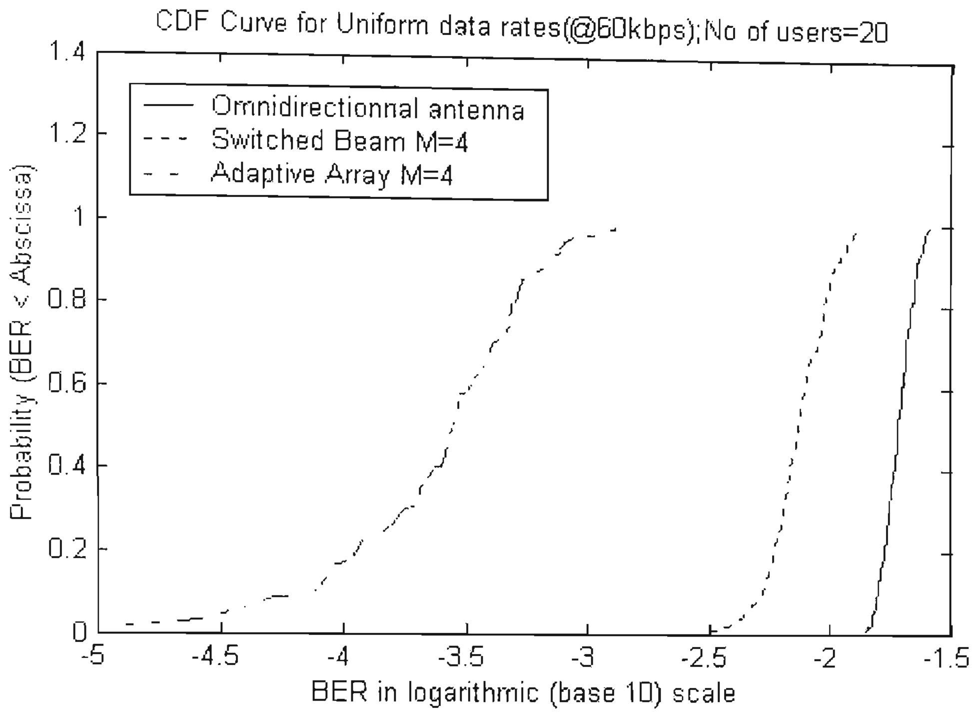

Figure 6.5: The CDF curves for omni directional, switched beam and adaptive array antennas.

6.2.3 Beam Patterns

A beam pattern was obtained for the 4 element-adaptive antenna arrays and the plot is given in Fig. 6.6. The angle of arrival (AOA) of the desired user is 90 deg. and the number of users is 5 respectively. The AOA's of the other users (interferers) were assumed to be randomly distributed between 30 deg. and 150 deg. (hence a 120 deg. sector) The other parameters used are the same as before (Table 6.1).

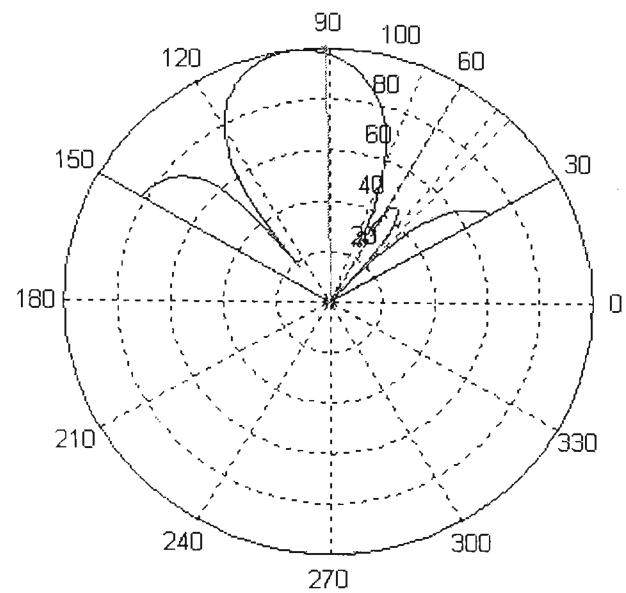

Figure 6.6: The Beam pattern for the adaptive antenna array.

Similarly, a beam pattern for the switched beam array was plotted as shown in Fig. 6.7. The number of users is 5 and the AOA of the desired user is 90 deg.

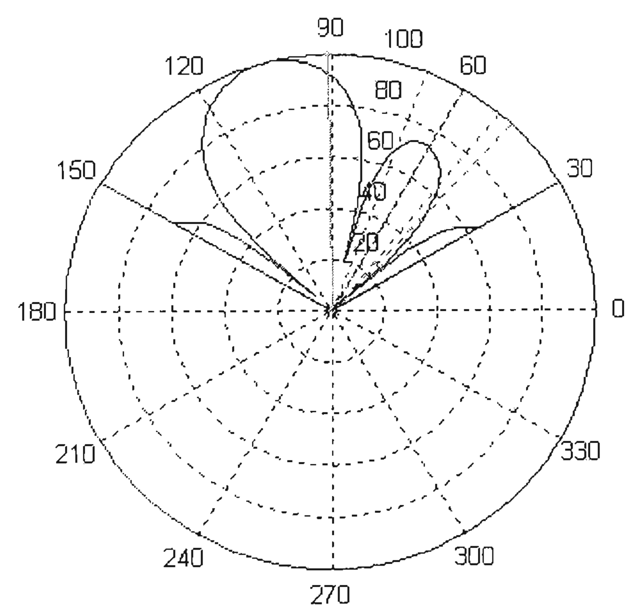

Figure 6.7: The Beam pattern for the switched beam antenna.

From Fig. 6.6 and Fig 6.7, it can be seen that the main beam of the adaptive antenna array focuses more on the desired user and the nulls towards the interferers compared with the switched beam antenna. This explains the performance gain of the adaptive array system.

Similarly, simulations were carried out for eight-element antenna systems (switched beam and adaptive array) in comparison with the omni directional antenna, and the BER results are presented in Fig.6.8. Figs 6.9 and 6.10 depict the beam patterns for both switched beam and adaptive array antennas of the eight element systems. From the beam patterns of both systems, we can see that beams are narrower and more focused towards the desired user in comparison with the four-element case. Furthermore, it is easy to see that the performance of the adaptive array is again better than that of the switched beam array.

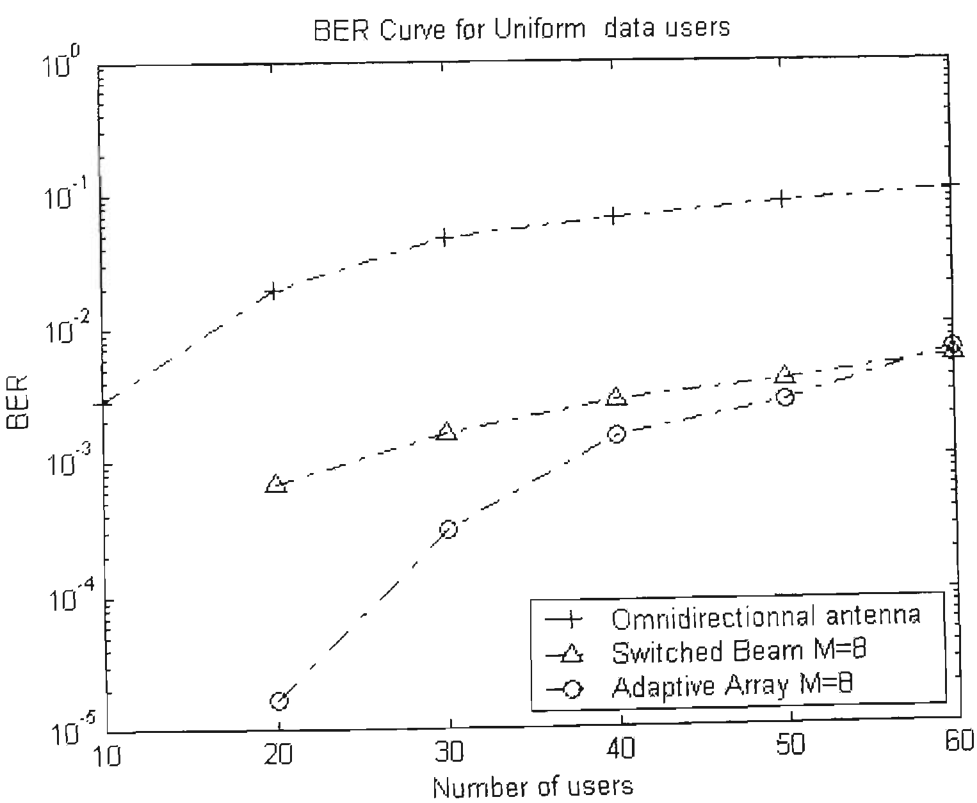

Figure 6.8: The BER's for uniform data users (8 elements).

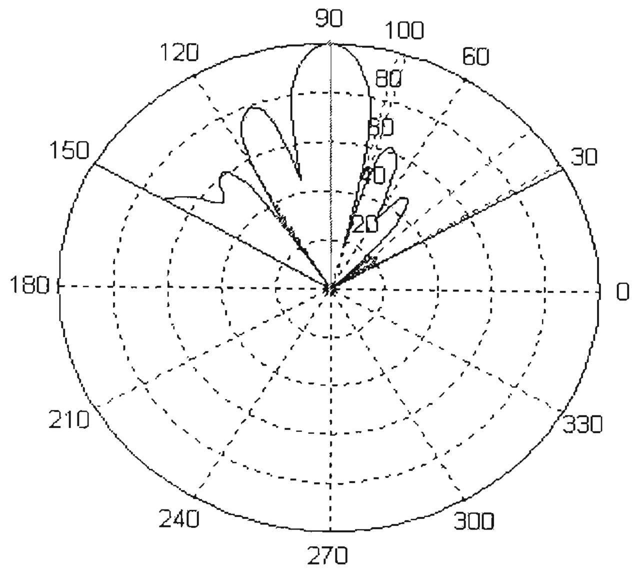

Figure 6.9: The Beam pattern for the adaptive antenna array.

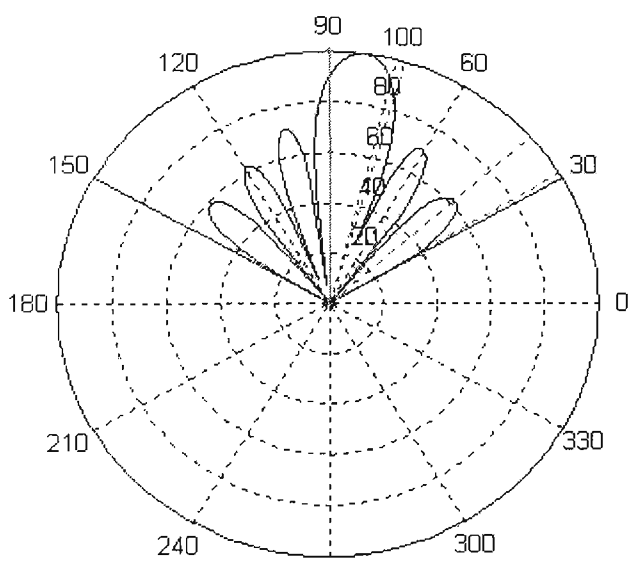

Figure 6.10: The Beam pattern for the switched beam antenna array.

6.2.4 Pole Capacity[1]

To determine the number of users that each antenna type can support within the 120 deg. sector in terms of pole capacity at a fixed threshold of bit error rate (10^{-2} is used in the simulations), the simulation program for the uniform data rate case was run by varying the value of E_b/N_0 from 0 to 14 dB. The results are shown in Fig.6.11.

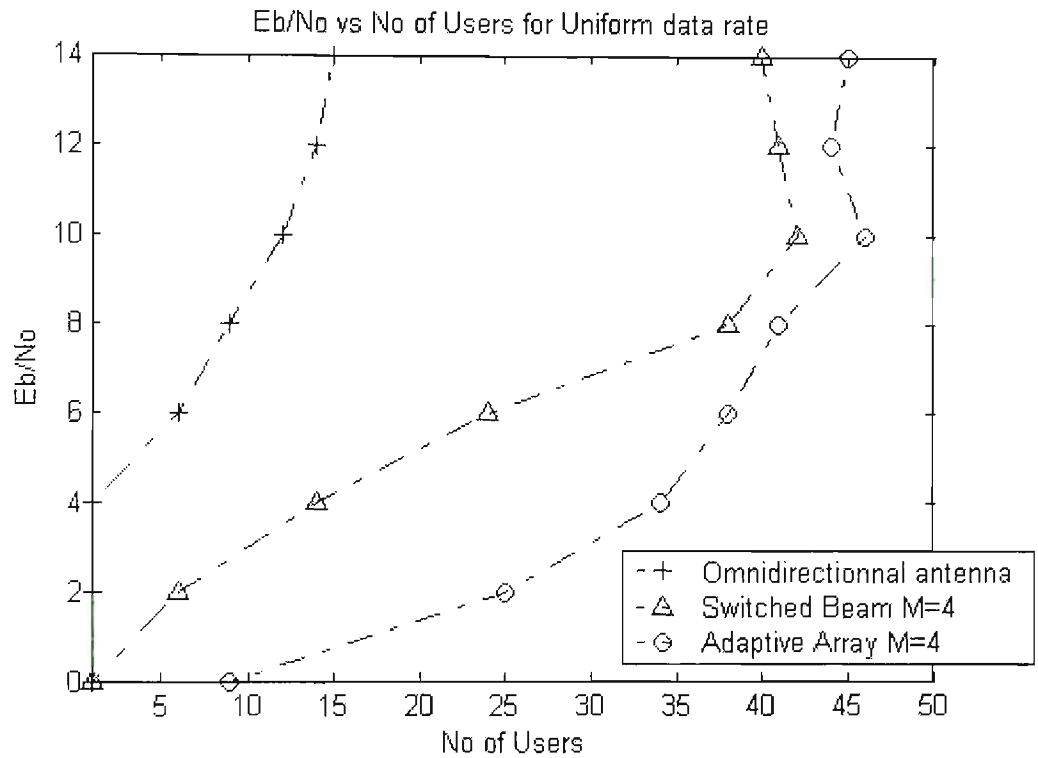

Figure 6.11: Pole Capacity for uniform data rate.

The pole capacity for each antenna type can be approximated by finding the highest number of users on the X-axis corresponding to the almost vertical part of each curve in Fig.6.11. As we can see, the pole capacity of the adaptive antenna array is approximately 45 compared with those of SB array and omni directional antennas, which has a pole capacity of approximately 40 and 15 respectively.

[1] Pole capacity is defined as the maximum number of users that an antenna type can support for a given condition.

6.3 BER's for Non-Uniform Data Rate Systems

In the previous sections, BER's were obtained for users with uniform data rate at 60kbps (both desired user and interferes). The graphs in this section illustrate the BER's for users transmitting at non-uniform data rates at 960kbps and 60kbps. For simplicity, one interferer was assigned as a high data rate user at 960kbps and other users including the desired user were assigned as low data rate users at 60 kbps to study the impact of the higher interference that the higher data rate user will create on the other uniform data rate users. Also, the angles of arrival of the high data rate user and the desired user were assumed to be 80 deg. and 90 deg. respectively.

6.3.1 Four-Element Antenna Arrays

The simulation results were obtained for the adaptive antenna array and the switched beam antenna array when the number of elements of each array is 4. The curve showing BER vs. number of users is shown in Fig.6.12.

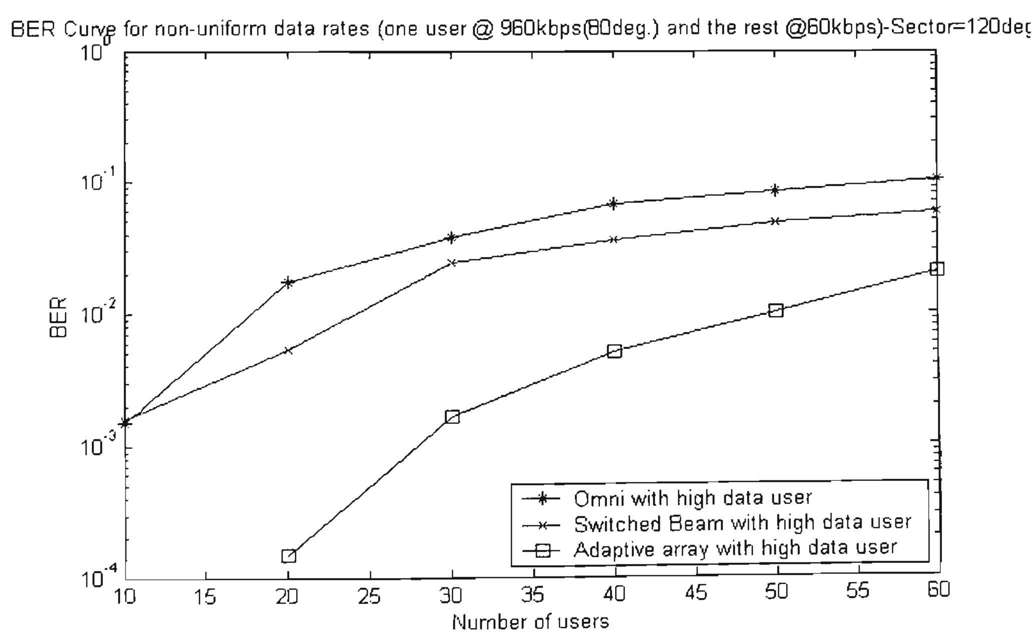

Figure 6.12: The BER's for four element antenna systems.

The PDF and CDF curves for the above non-uniform data rate case are shown in Fig. 6.13 and Fig. 6.14, respectively, with number of users=20. Compared with Fig. 6.4 and Fig. 6.5, a much greater BER improvement has clearly been achieved in this non-uniform case than that in the uniform data rate case. This exactly demonstrates the enormous performance potential of adaptive arrays in the context of 3G (i.e., non-uniform traffic).

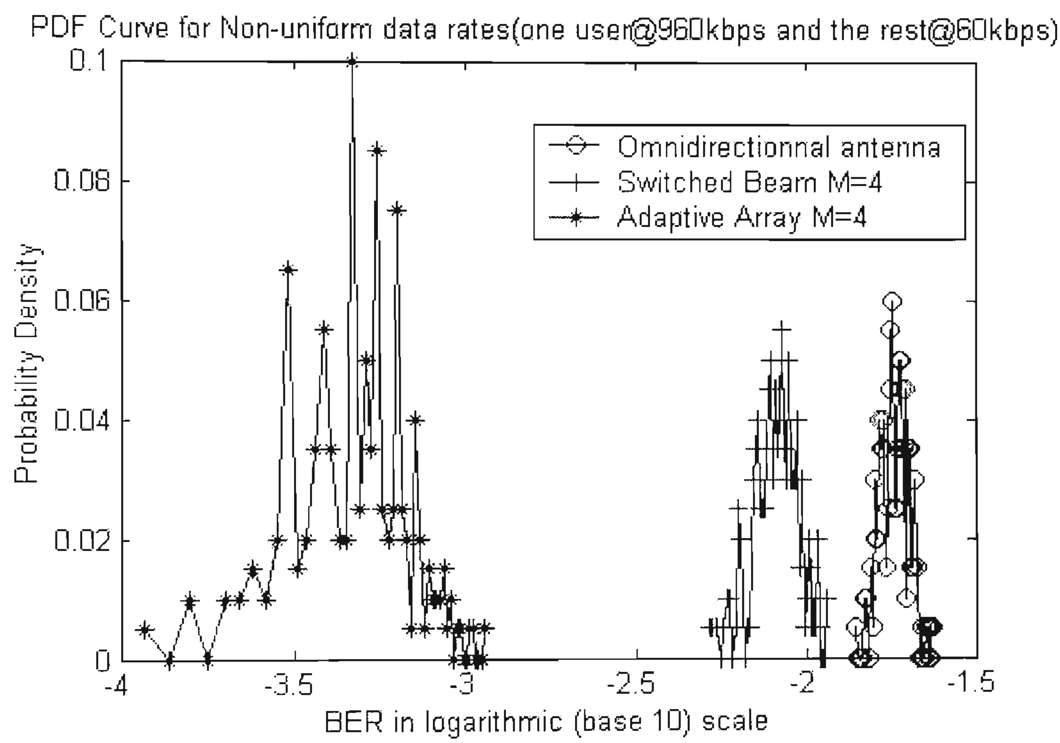

Figure 6.13: The PDF curves for omni directional, switched beam and adaptive array antennas.

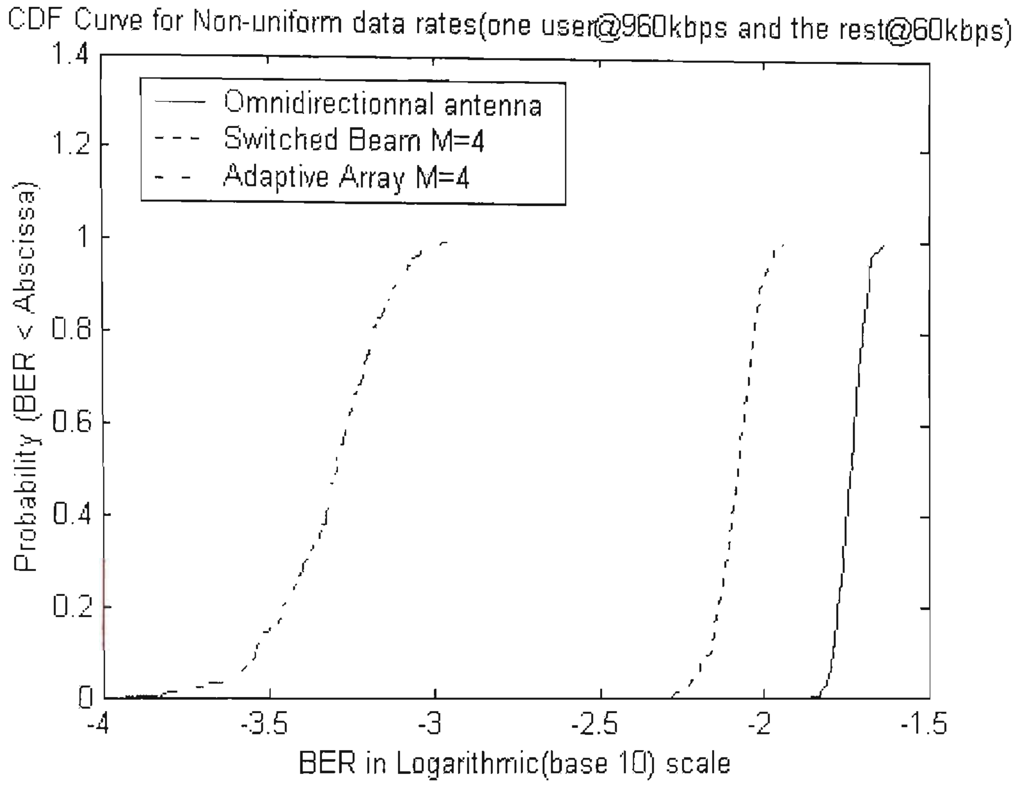

Figure 6.14: The CDF curves for omni directional, switched beam and adaptive array antennas.

The beam pattern for the adaptive arrays (4 elements) was plotted in Fig. 6.15 (the number of users=5). The dotted lines indicate the angle of arrival of each user.

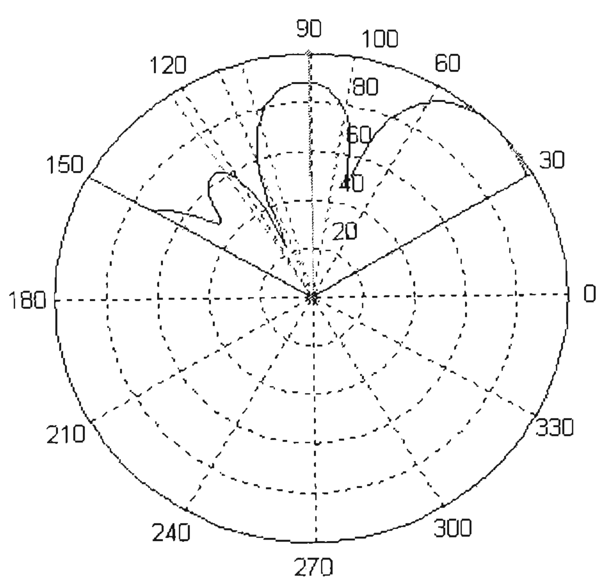

Figure 6.15: The Beam pattern for the adaptive antenna array.

Similarly, the beam pattern for the switched beam antenna is drawn in Fig. 6.16 below for comparison purposes.

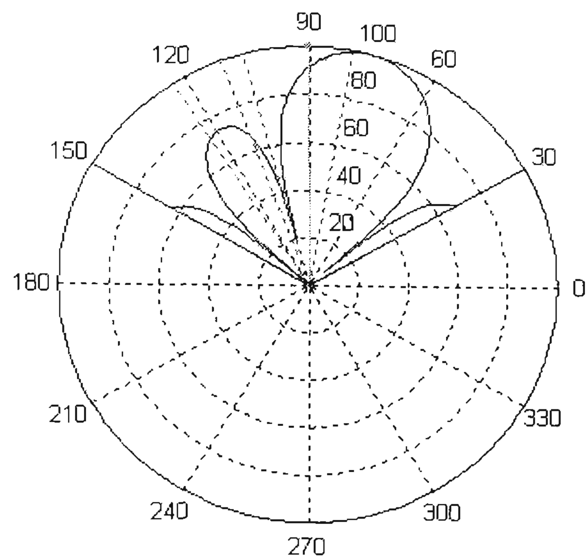

Figure 6.16: The Beam pattern for the switched beam antenna array.

Similar to Fig.6.11, the pole capacity curves for the non-uniform data rate scenario have been plotted in Fig.6.17. As defined in section 6.2.4, the pole capacity for each antenna system was found from the graph in Fig. 6.17 and found that the pole capacity of the adaptive array antenna significantly outperformed the SB array and omni directional antennas in a non uniform data rate case.

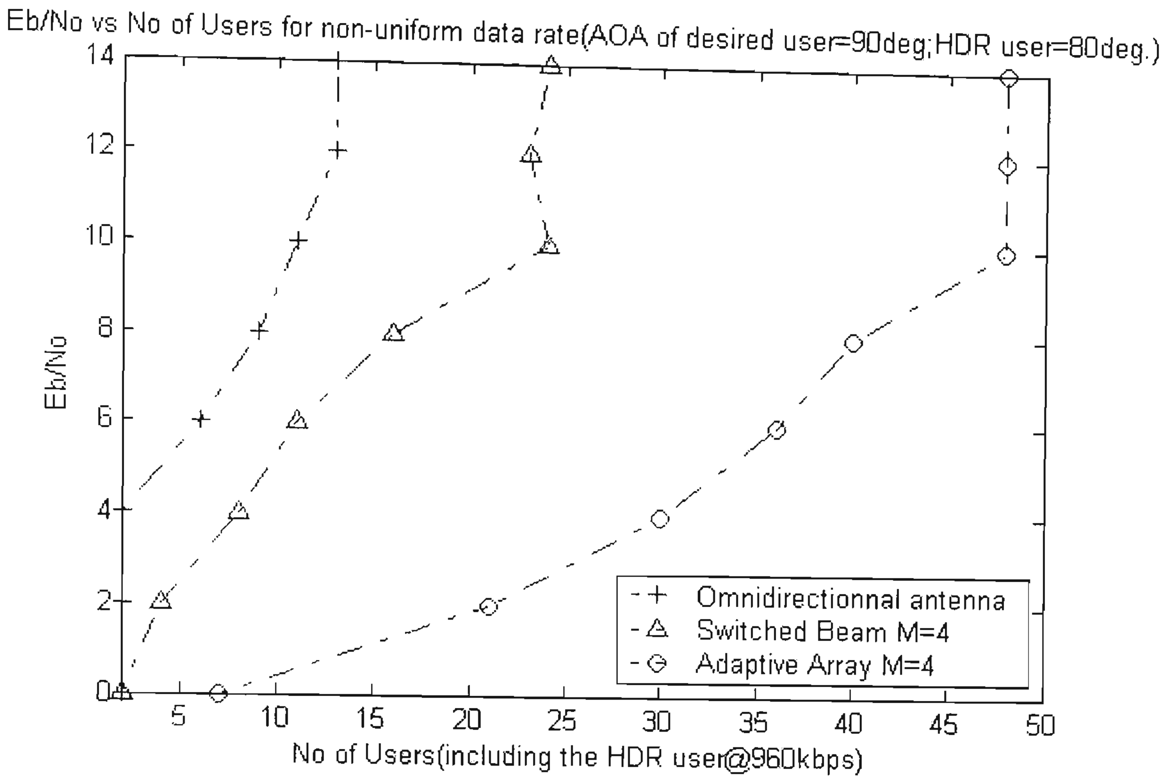

Figure 6.17: Pole Capacity for non-uniform data rate.

6.3.2 Eight-Element Antenna Arrays

Similar simulations were conducted for the 8-element antenna system. The corresponding BER's are plotted in Fig.6.18. It can be seen that the BER performance for the adaptive array significantly increases with the increase of the number of elements whereas switched beam antenna performance follows the same trend with a slight increase.

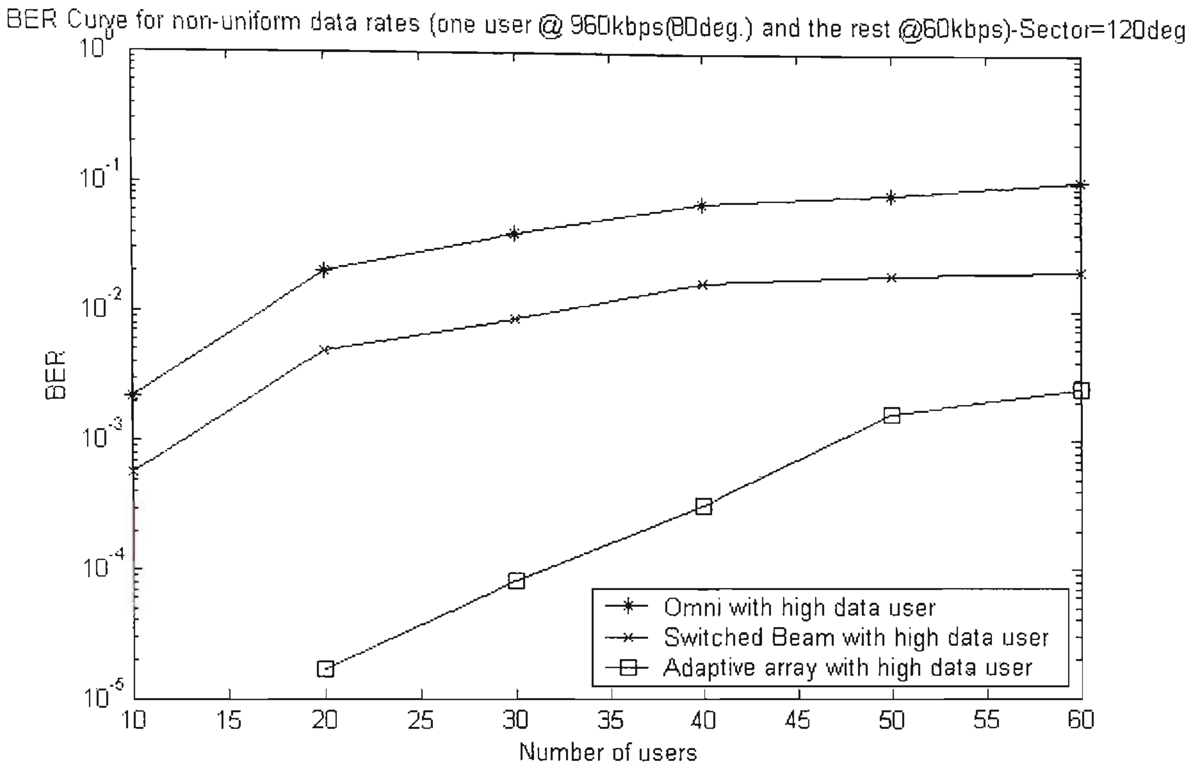

Figure 6.18: The BER's for eight element antenna systems.

The PDF and CDF curves in Fig. 6.19 and 6.20 depict the BER performance of the omni directional, switched beam and adaptive array antennas for the non-uniform data rate case illustrated in Fig. 6.18. As we can see from the PDF and CDF curves, BER distribution of the adaptive array is narrower compared with the other two antenna systems. Compared with Fig. 6.8, these results again indicate a high performance gain of the adaptive array in the non-uniform case.

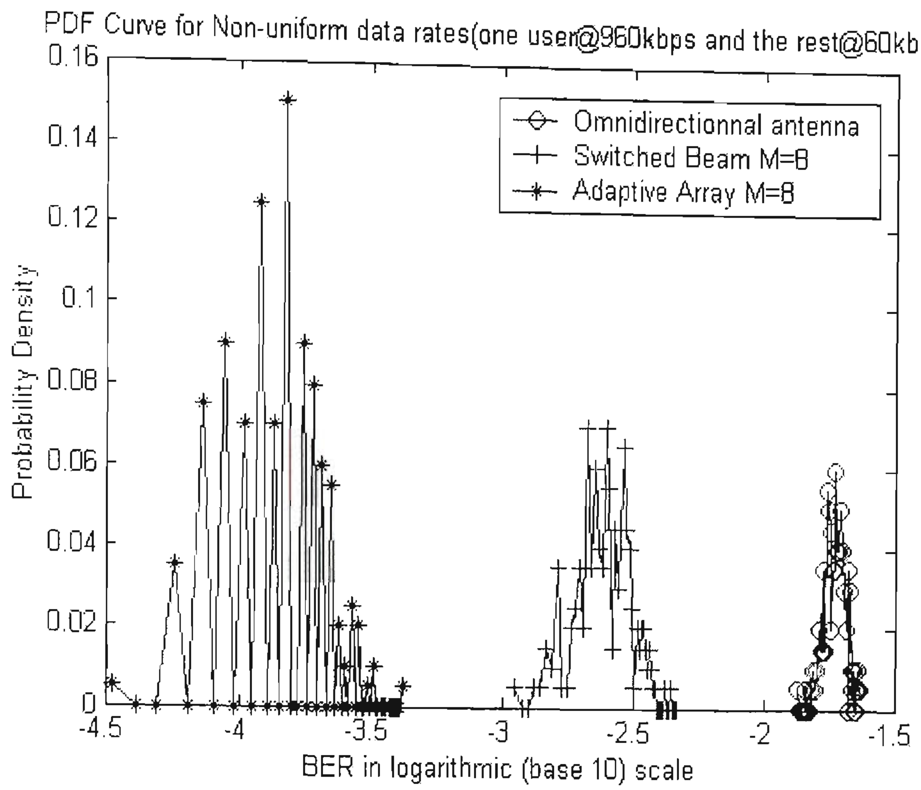

Figure 6.19: The PDF curves for omni directional, switched beam and sdaptive array antennas.

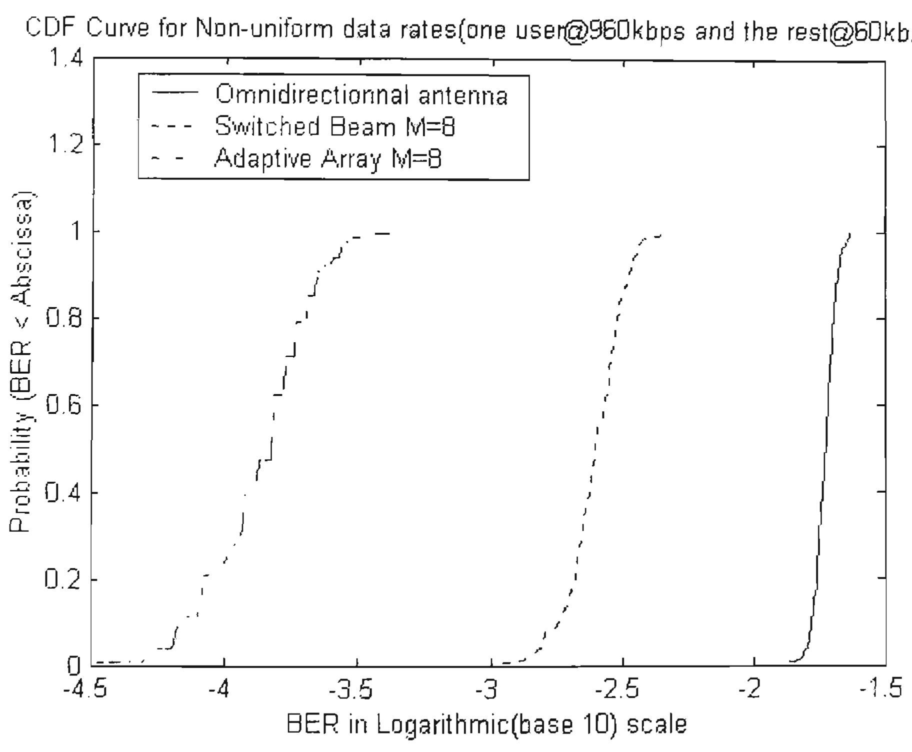

Figure 6.20: The CDF curves for omni directional, switched beam and adaptive array antennas.

The beam pattern for the 8 element adaptive antenna is plotted in Fig. 6.21 when the number of users is 5. The dotted lines indicate the angle of arrival of each user.

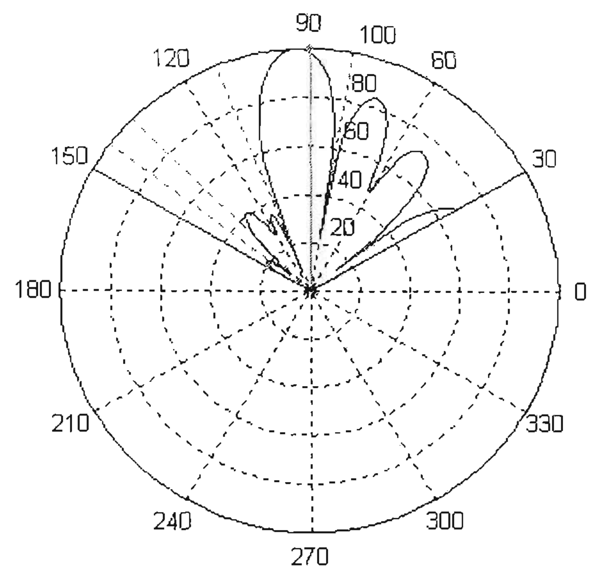

Figure 6.21: The Beam pattern for the adaptive antenna array.

Similarly, the beam pattern for the switched beam antenna is presented in Fig. 6.22 for comparison.

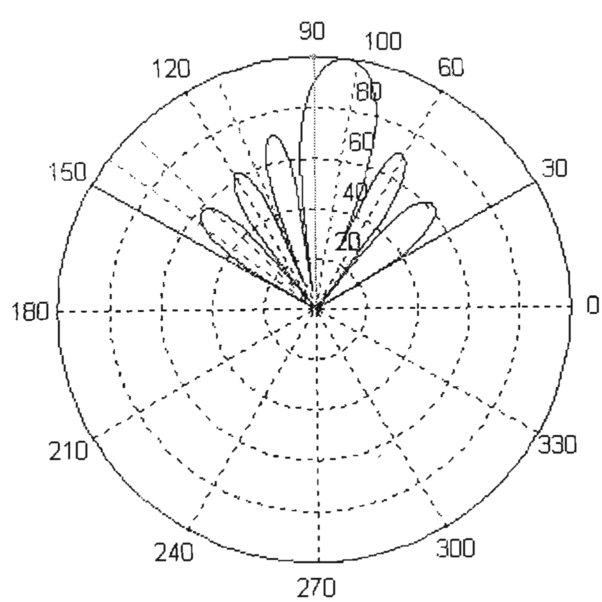

Figure 6.22: The Beam pattern for the switched beam antenna array.

Finally, the BER performances of the antenna systems shown in Fig. 6.12 (four element case) and Fig. 6.18 (eight element case) are plotted together in Fig. 6.23 for comparison purposes. We can clearly see from the plot below that BER performance of each antenna system decreases with the increase of number of interferers. Also, for a given BER, both switched beam and adaptive array systems allow more interferers with the increase of number of elements from four to eight. The BER vs. number of users of a single (omni) antenna is also shown in the plot as a reference.

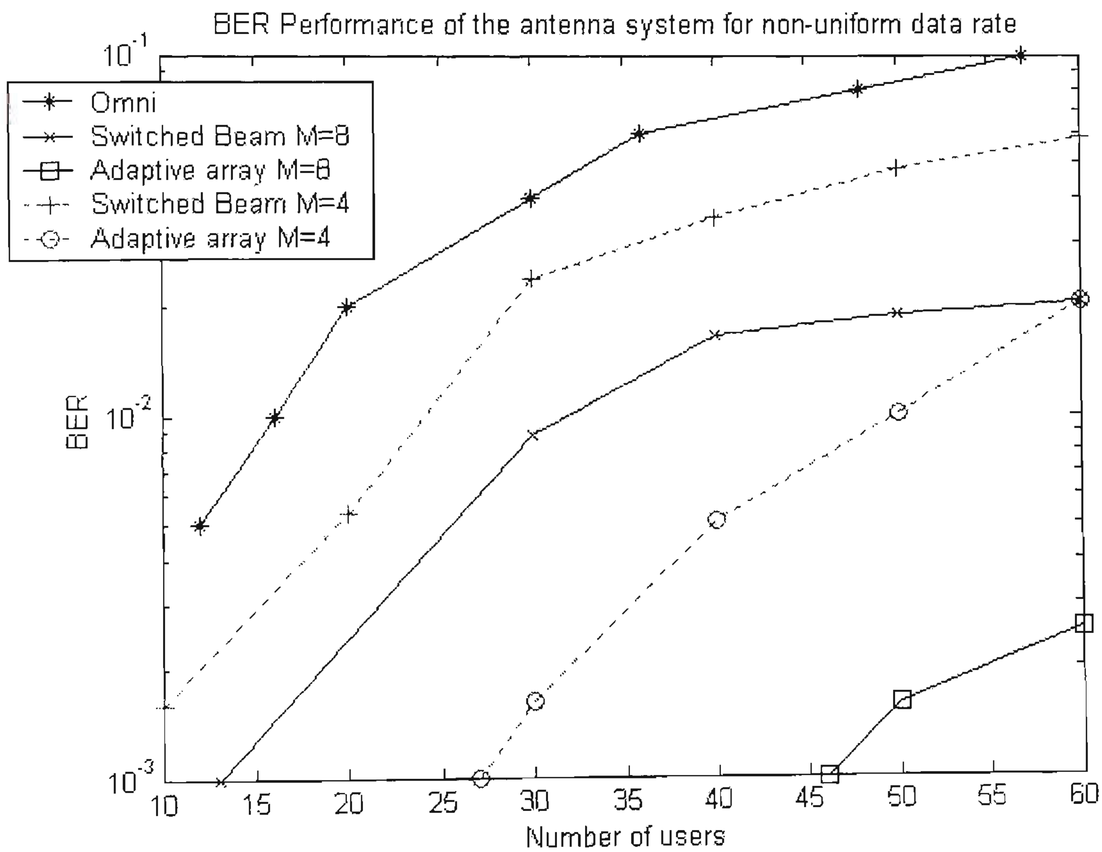

Figure 6.23: Comparison of BER's for four and eight element antenna systems.

6.4 Modification of the Simulation Model

In this section, an attempt has been made to make the simulation model more realistic by adding the following two segments into the main simulation model: (1) time varying channels, and (2) the Q channel based adaptive algorithm.

6.4.1 Time Varying Channels

The Rayleigh fading model developed in Section 4.3.2 was introduced into the simulation model between the transmitter and the receiver. The output signal coming out of the transmitter is multiplied by the output of the fading channel module before arriving at the receiving antenna system. Fig.6.24 shows the BER performance against number of interferers for omni directional, switched beam and adaptive array antenna systems at a uniform data rate of 60kbps, and Fig.6.25 depicts the results of the non-uniform rate case (with a high-rate user of 960kbps). The angles of arrival of all users are randomly selected within 120 deg. and the number of antenna elements is 4 for the adaptive and the switched beam antenna arrays. As we can see from Fig. 6.24 and 6.25, the adaptive array antenna offers a higher robustness against Rayleigh fading compared with SB array and omni directional antenna systems.

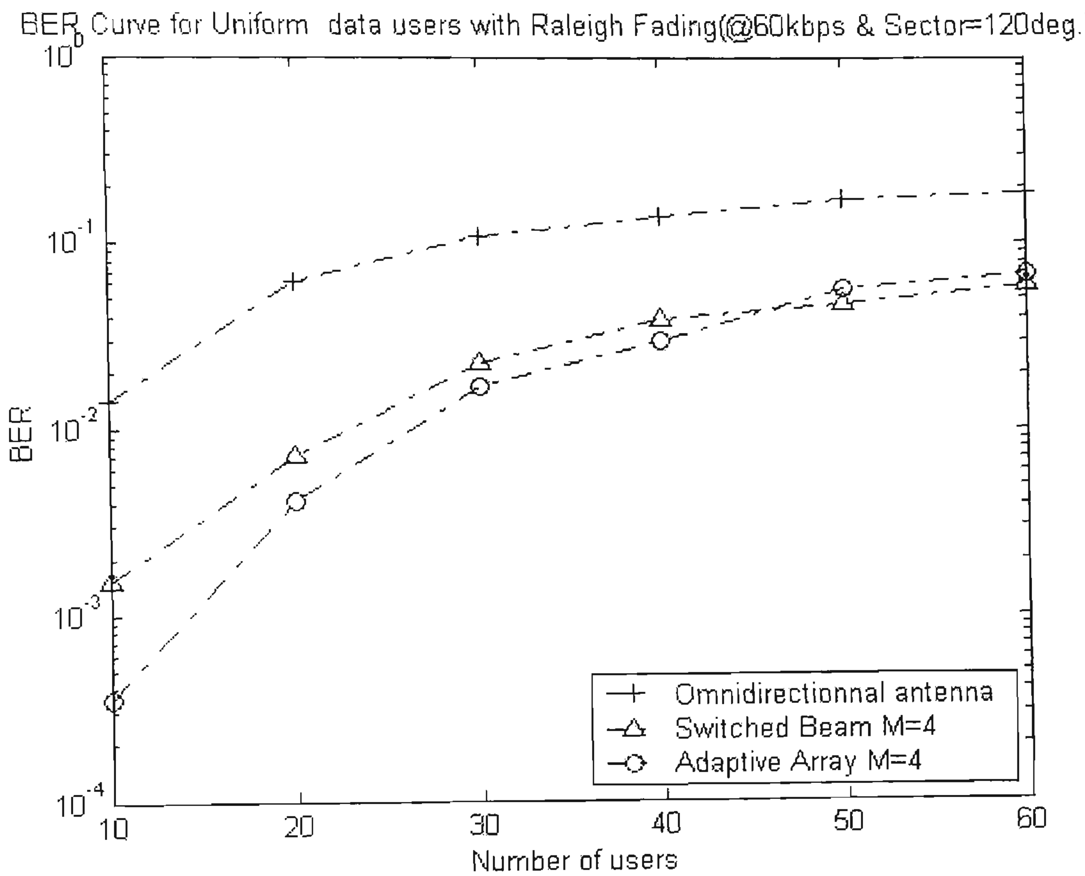

Figure 6.24: The BER for uniform data users with Rayleigh fading.

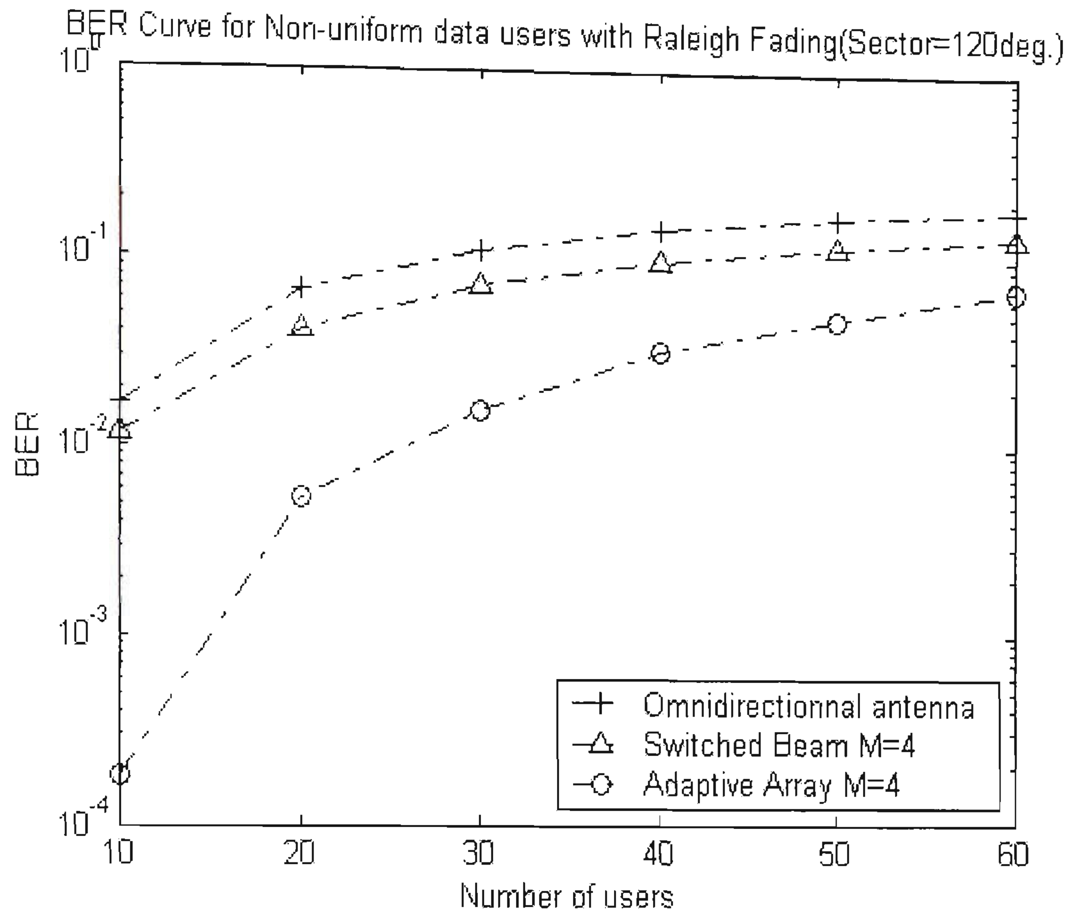

Figure 6.25: The BER for non-uniform data users with Rayleigh fading.

6.4.2 The Q channel Based Adaptive Algorithm

The results generated so far utilized both Q & I channel signals to find the optimum weight vector for the adaptive algorithm. In this section, we use only Q channel information in the optimization process. The following results show the impact of Q channel on the BER performance of the adaptive algorithm. The parameters used for the simulation are the same as in section 6.3.1 (non-uniform data rate for four element antenna). It is noted from Fig. 6.26 that the performance of the adaptive array has decreased slightly when only Q channel is used compared with the case in section 6.3.1 when both I and Q channels are used. The reason for the poorer performance is that more information and energy are available in the I+Q channel case than in the Q channel-only case in the optimization process.

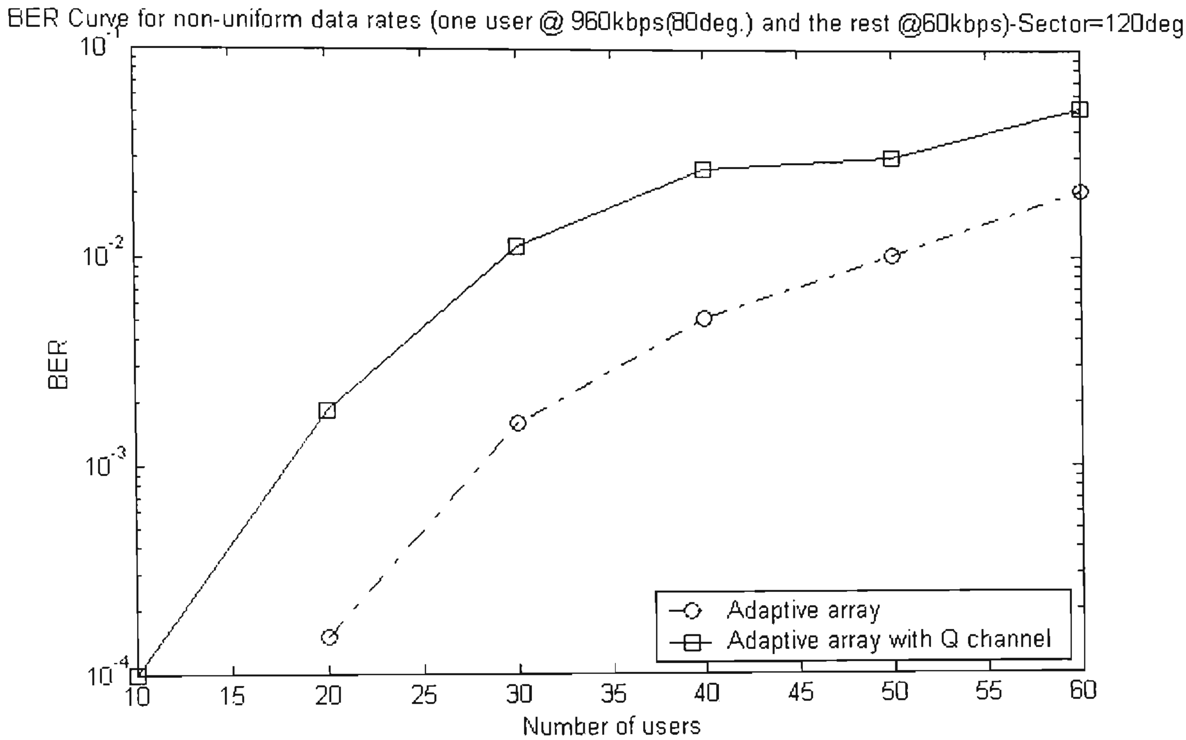

Figure 6.26: The BER for non-uniform data users with Q channel based adaptive array.

The PDF and the CDF curves for non-uniform data users (with Q channel only) are shown in Fig. 6.27 and Fig. 6.28, respectively. The CDF curves also show that BER performance of the adaptive array with Q channel is slightly worse than the adaptive array with I and Q channels. However, both curves for the adaptive array follow a similar pattern.

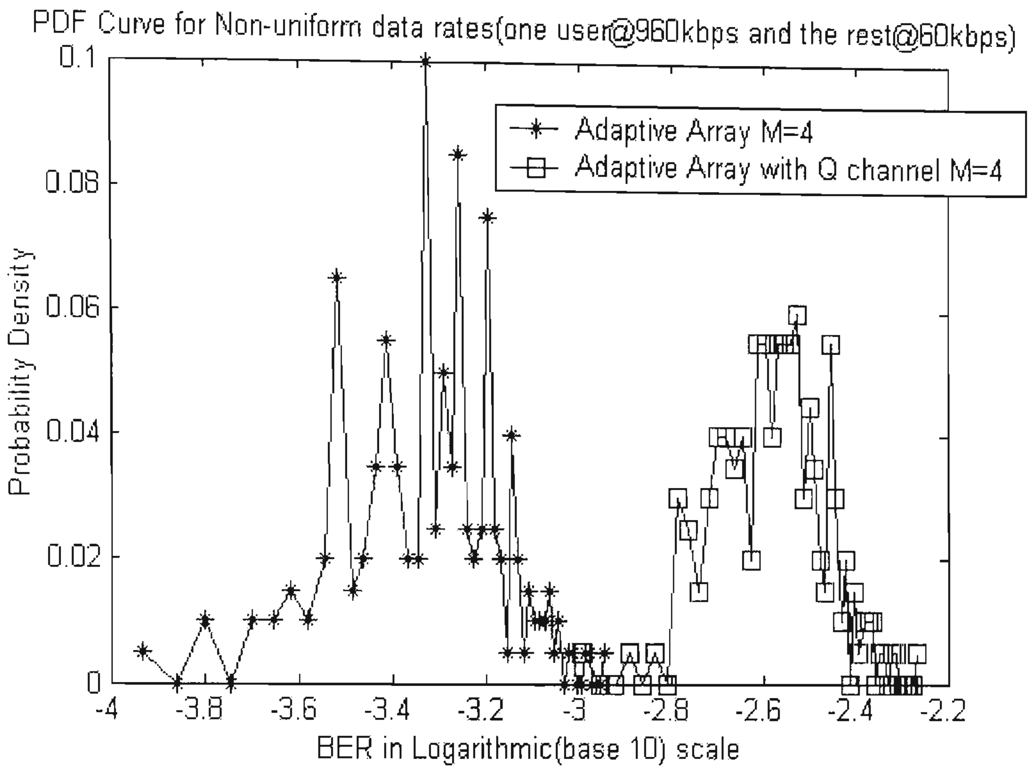

Figure 6.27: The PDF curves for adaptive array antennas.

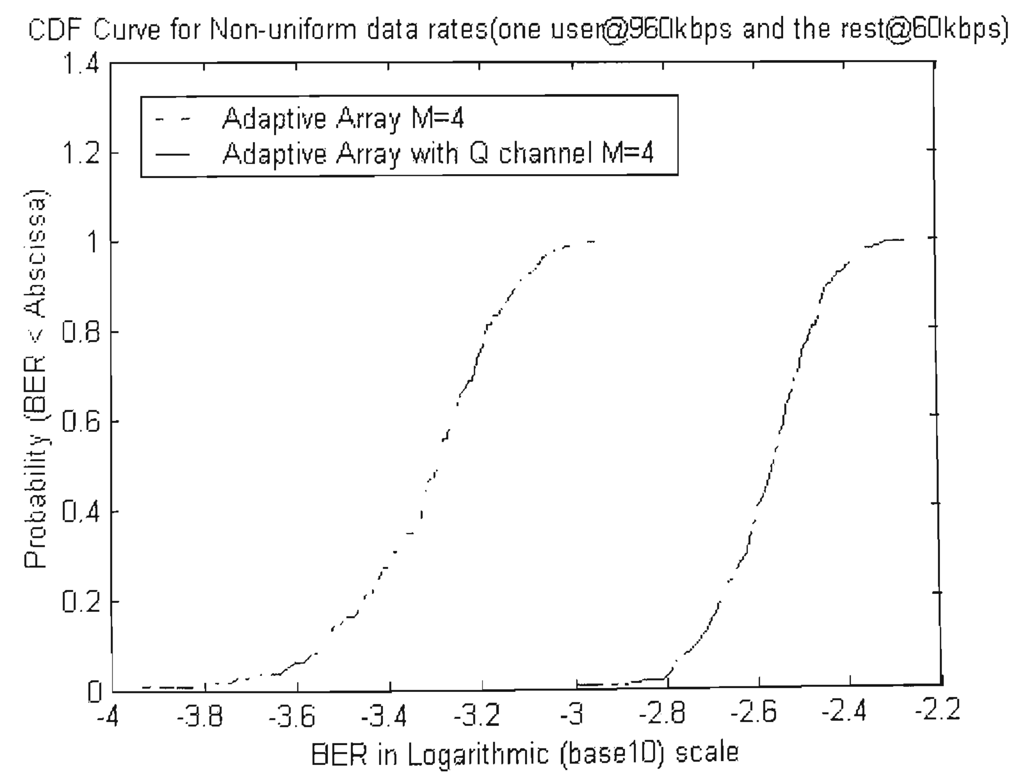

Figure 6.28: The CDF curves for adaptive array antennas.

6.5 BER's for Lagrange Multiplier (LM) Based Adaptive Algorithm

The BER's for the desired user against the number of interferers were obtained both for the omni directional antenna and for the adaptive array antenna. The parameters for the uplink simulation program are the same as used before (Table 6.1).

In this study, we also use Q channel information only in the optimisation process. Fig. 6.29 illustrates the BER performance for users transmitting at non-uniform data rates of 960kbps and 60kbps. As before, for simplicity, one interferer was assigned as a high data rate user at 960kbps and all the other users including the desired user were assigned as low data rate users at 60 kbps and 15 kbps. Similarly, the angles of arrival of the high data rate user and the desired user were assumed to be 80 deg. and 90 deg. respectively.

Fig. 6.30 shows the BER performance of the omni directional and adaptive antenna systems against E_b/N_o when the total number of users=10. It can be noticed from the graph that the adaptive array still offers a significant performance gain although the BER's of both systems improve as E_b/N_o varies from 2-18 dB.

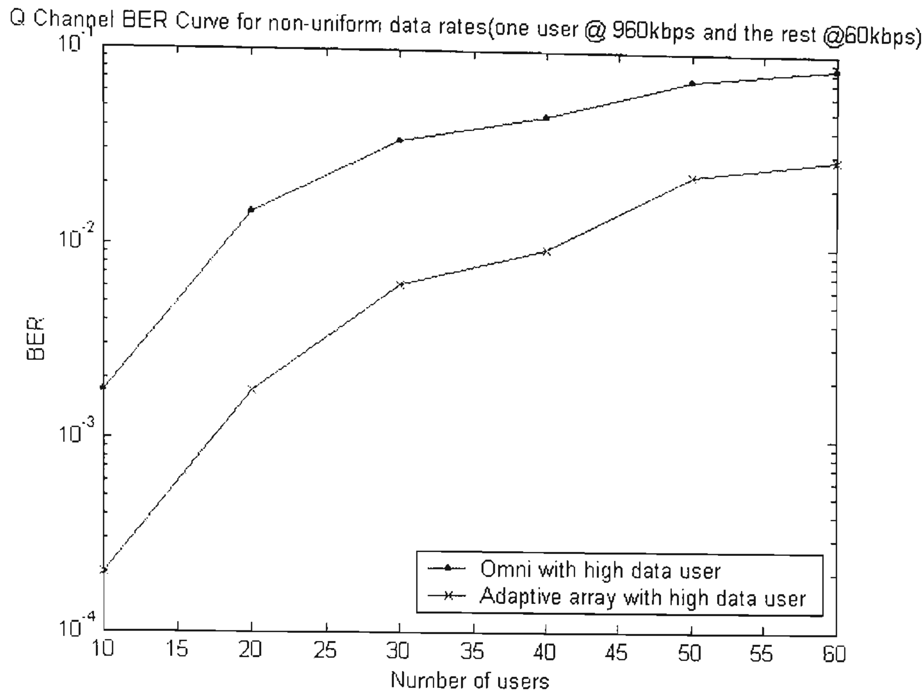

Figure 6.29: The BER's of an omni directional antenna system and an adaptive array system based on Q channel only in a mixed data rate environment.

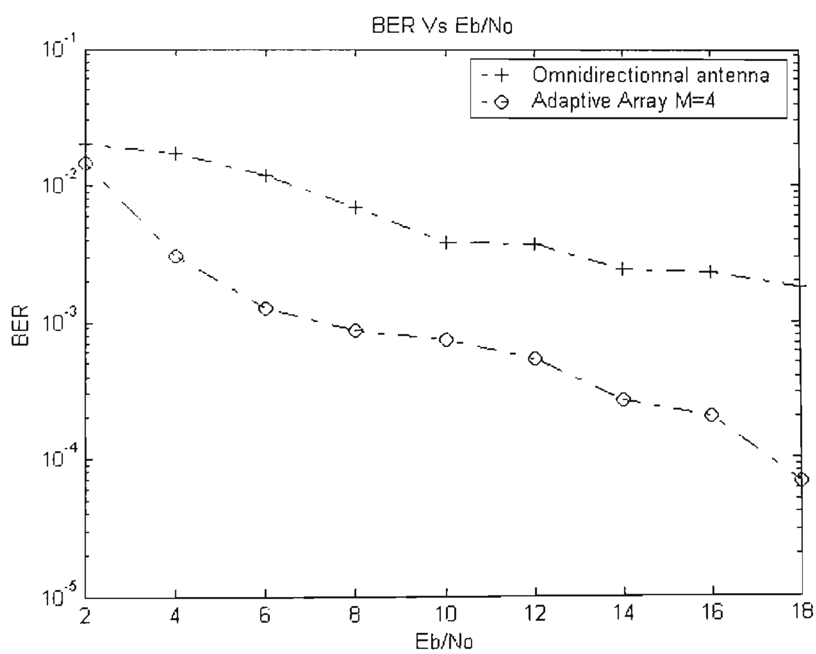

Figure 6.30:The BER's of an omni directional antenna system and an adaptive antenna system based on Q channel only in a mixed data rate environment (total number of users=10).

In this Chapter, we used mainly two beamforming algorithms; LS-DRMTA and LM method, to generate the simulation results. The results were presented in terms of BER vs. number of users and BER's vs. E_b/N_0. When we compare the performances of both techniques (Fig. 6.12 and Fig. 6.29) in a non-uniform data rate environment, it can be noticed that LS-DRMTA shows slightly better results. However, we also observed that LM is a more effective method as the number of iterations required to obtain the optimum weight vector is extremely low compared with the LS-DRMTA method. Finally, we suggest that it will be worthwhile to combined LS-DRMTA and LM to obtain an even better performance.

Chapter 7

Conclusion and Future Work

This thesis has presented a basic smart antenna simulation program for WCDMA in the FDD mode for uplink transmission. The major modules of the simulation program have been described in detail: the transmitter, receiver and the channel model. The simulation results are presented in (1) BER, (2) radiation patterns, (3) PDF and CDF formats, and (4) pole capacity, both for the uniform data rate systems and for the non-uniform data rate systems. In addition, we investigated the BER performance of the antenna systems (Omni, switched beam and adaptive array antennas) with time varying channels and adaptive algorithms with Q-channel only. The main results can be summarized as follows.

For the uniform rate case, the BERs for the adaptive array are better than those of the switched beam array for a low number of users. Therefore, a comparison of cost and complexity associated with the implementation of both systems must be carried out to identify which system suits better in a particular application. As was expected, we also noticed that BERs become better with the increment of the number of elements (both uniform and no-uniform cases). In applications, however, this number is normally kept below eight elements due to cost and practical reasons.

Most importantly, in the non-uniform data case, we observed much better results with the adaptive array system using both LS-DRMTA and Lagrange multiplier method. This exactly confirmed the theoretical prediction: Smart antenna are much more suitable for the 3G CDMA system (with mixed traffic) than for the 2G CDMA system (with uniform traffic).

The following assumptions were used in the simulation part of this research and further work is suggested to make the simulation model to be more realistic.

- Simulated users are scattered within a sector (120 deg.) in such a way that their received power levels at the base station are within the threshold power level (+/- 2 dB) targeted by the base station: Distribution of the users can be re-modeled as in a real mobile user environment and distance to the user from the base station should also be factored into the simulations.

- Uplink transmission (Mobile to Base station) for FDD only: This can be extended to include downlink transmission (Base station to Mobile), especially for the TDD mode of UTRA.

- The Transmit-receive system has a perfect power control: Performance can be analyzed by introducing an imperfect power control mechanism to the transmit-receive system.

- Only one Rake finger is considered: Further research is required to extend the current simulator for a multiple rake receiver.

References

[1]. M. Chryssomallis, N.Herscovici and C. Christodoulou, "Smart Antennas," *IEEE Transactions on Antennas and Propagation*, Vol. 42, No. 3, pp.129-136, June 2000.

[2]. J.C. Liberty and T.S. Rappaport: *Smart Antennas for Wireless Communications – Principle and Practice*, Prentice Hall, NJ, 1999.

[3]. Malcom W. Oliphant, "The mobile phone meets the internet," *IEEE Spectrum*, pp.20-28, August 1999.

[4]. T.S. Rappaport: *Wireless Communications – Principle and Practice*, Prentice Hall, NJ, 1996.

[5]. Third Generation Partnership Project: *Technical Specification Group Radio Access Network - Spreading and Modulation*, TS 25.213V2.1.1(1999-4).

[6]. J.H. Winters, "Smart Antennas for Wireless Systems," *IEEE Personal Communications*, pp.23-27, February 1998.

[7]. B. Widrowl, P.E. Mantey, L.J. Griffiths and B.B. Goode, "Adaptive Antenna Systems," *Proc. of IEEE*, Vol. 55, pp. 2143-2161, December 1967.

[8]. G. V. Tsoulos et al, "Performance Enhancement of DS-CDMA Micro cellular Networks with Adaptive Antennas," *In the proceedings of the IEEE Vehicular Technology Conference*, pp. 1086-1090, April 1996.

[9]. R. B. Ertel, P. Cardieri, K.W. Sowerby, T.S. Rappaport and J.H. Reed, "Overview of Spatial Channel Models for Antenna Array Communication Systems," *IEEE Personal Communications*, pp. 10-22, February 1998.

[10]. S. Kwon, I. Oh and S. Choi, "Adaptive Beam forming from the Generalized Eigenvalue problem with a linear complexity for a wideband CDMA channel," *In the proceedings of the IEEE Vehicular Technology Conference*, pp.1890-1894, 1999/Fall.

[11]. F. Alam, D. Shim and B. D. Woerner, "The performance of a Rake Receiver for WCDMA Mobile Communications System", *In the proceedings of IEEE Vehicular Technology Conference*, Vol. 1, pp. 521-525, October 2001.

[12]. F. Alam, K. A. Zahid, B.D. Woerner and J. H. Reed, "Performance Comparison between Pilot Symbol Assisted and Blind Rake-Rake Receivers at the Reverse Link of CDMA System", *In the proceedings of IEEE Vehicular Technology Conference*, Vol.1, pp. 353-357, October 2001.

[13]. Y. M. Vasavada, T.E. Biedka, J.H. Reed, " Code Gated Algorithm: A Blind Adaptive Antenna Array Beam forming Scheme for Wideband CDMA," *In the proceedings of the Thirty-forth Asilomar conference on Signals, Systems and Computers*, Vol.2, pp. 1397-1402, November 2000.

[14]. T. K. Sarkar, J. Koh, R. Adve, R.A. Schneible, M.C. Wicks and S. Choi, "A Pragmatic Approach to Adaptive Antennas," *IEEE Transactions on Antennas and Propagation*, Vol.42, No. 2, pp. 39-55, April. 2000.

[15]. F. Adachi, M. Sawahashi and H. Suda, "Wideband DS-CDMA for Next-Generation mobile Communications Systems," *IEEE Communications Magazine*, September 1998.

[16]. S. Ponnekanti, "An Overview of Smart Antenna Technology for Heterogeneous Networks," *IEEE Communications Surveys Magazine*, Vol. 2, No. 4, pp. 14-23, Forth Quarter 1999.

[17]. P. H. Lehne and M. Pettersen, "An Overview of Smart Antenna Technology for Mobile Communications Systems," *IEEE Communications Surveys magazine*, Vol. 2, No. 4, pp. 2-13, Forth Quarter 1999.

[18]. B. Allen, M. Beach and P. Karlsson, "Analysis of Smart Antenna Outage in UTRA FDD Networks," *Electronic Letters*, Vol. 38, No. 1, pp. 2-3, January 2002.

[19]. M. Beach, B. Allen and P. Karlsson, " Spatial De-correlation of frequency Division Duplex Links," *Electronic Letters*, Vol. 36, No. 22, pp. 1884-1885, October 2000.

[20]. F. Adachi and M. Sawahashi, " Wideband Multi-rate DS-CDMA for Next Generation Mobile Communication Systems," *IEEE Wireless Communication Conference*, May 1997.

[21]. F. Alam, D. Shim and B. D. Woerner, " A New Low-Complexity Rake Receiver for WCDMA," *In the proceedings of IEEE Vehicular Technology Conference*, Vol. 1, pp. 160-164, May 2002.

[22]. T. Ojanpera and R. Prasad: *WCDMA: Towards IP Mobility and Mobile Internet*, Artech House, 2001.

[23]. F. Swarts et al: *CDMA Techniques for Third generation Mobile Systems*, Kluwer Academic publishers, 1999.

[24]. J.B. Groe, L. E. Larson: *CDMA Mobile Radio Design*, Artech House, 2000.

[25]. J. S. Lee and L. E. Miller: *CDMA Systems Engineering Handbook*, Artech House, 1998.

[26]. S. choi and D. Yun "Design of an Adaptive Antenna Array for Tracking the Source of Maximum Power and Its Application to CDMA Mobile Communications," *IEEE Transactions on Antennas and Propagation*, Vol.45, No. 9, pp. 1393-1404, September 1997.

[27]. L. J. Griffiths, "A Simple Adaptive Algorithm for Real-Time Processing in Antenna Array," *Proc. of IEEE*, Vol. 57, No. 10, pp. 1696-1704, October 1969.

[28]. G. V. Tsoulos, M. A. Beach and S. C. Swales, "DS-CDMA Capacity Enhancement with Adaptive Antennas," *Electronic Letters*, Vol. 13, No. 16, pp. 1319-1320, August 1995.

[29]. M. G. Kyeong and Y.G. Kang "Outdoor Communications Using Adaptive Arrays in CDMA Mobile Systems," *In the proceedings of IEEE Vehicular Technology Conference*, Vol. 1, pp. 264-268, May 1999.

[30]. 3GPP: *Technical Specifications: Group radio access network*, V.3.1.1, Dec. 1999.

[31]. H Holma and A. Toskala: *WCDMA for UMTS – Radio access for third generation mobile communications*, Wiley, NY, 2001.

[32]. S.Choi and D.Yun, "Design of Adaptive Antenna Array for Tracking the source of Maximum Power and Its Application to CDMA Mobile Communications," *IEEE Transactions on Antennas and Propagation*, AP-45, No. 9, pp.1393-1404, September 1997.

[33]. S. Choi, D. Shim and T.K. Sarkar, "A comparison of Tracking-Beam Arrays and Switching-Beam Array Operating in a CDMA Mobile Communication Channel," *IEEE Transactions on Antennas and Propagation*, Vol. 41, No. 6, pp.10-22, December, 1999.

[34]. D. Shim and S. Choi, "A New Blind Adaptive Algorithm Based on Lagrange's Formula for a Real-Time Design of a Smart Antenna,"*In the Proceedin. of IEEE Vehicular Technology Conference*, Vol. 3, pp. 1660-1664,Ottawa, Ontario, Canada, 1998.

[35]. K. Watanabe, I. Yoshii and R. Kohno, " An Adaptive Array Antenna Using Combined DFT and LMS Algorithms," *In the Proceedings of the ninth IEEE International Symposium on Personal Indoor and Mobile Radio Communications*, Vol.3, pp. 1417-1421, September 1998.

[36]. N. Herscovici and C. Christodoulou, " Potentials of Smart Antennas in CDMA Systems and Uplink Improvement," *IEEE Transactions on Antennas and Propagations*, AP-43, 5, pp.172-177, October 2001.

[37]. F. Alam, Simulation of Third Generation CDMA Systems (MSc Thesis). Virginia, USA: Virginia Polytechnic Institute and State University, 1999.

[38]. T. Ohganel, T. Shimura, N. Matsuzawa and H. Sasaoka, " An Implementation of a CMA Adaptive Array for High Speed GMSK Transmission in Mobile Communications," *In the Proceedings of IEEE Vehicular Technology Conference,* Vol. 42, No.3, pp.282-288, August 1993.

[39]. S.V. Schell et al., " Blind Adaptive Arrays for Increased Capacity in Cellular Communications,"*Wireless Personal Communications: Trends and Challenges, Ed.T.S. Rapapport, et al*, pp.16-26, Boston: Kluwer Academic, 1994.

[40]. B. Agee, "Blind Separation and Capture of Communications signals using a Multi-target Constant Modulus Beamformer," *IEEE Military Communications Conference*, Boston, MA, October, 1989.